A pilot project combining multispectral proximal sensors and digital cameras for monitoring tropical pastures

R. N. Handcock[1,*], D. L. Gobbett[2], L. A. González[3,#], G. J. Bishop-Hurley[4], and S.L. McGavin[3]

[1] Commonwealth Scientific and Industrial Research Organisation (CSIRO), Agriculture, Private Bag 5, Floreat, WA, 6014, Australia

[2] CSIRO Agriculture, PMB 2, Glen Osmond, SA, 5064, Australia

[3] CSIRO Agriculture, PMB Post Office, Aitkenvale, QLD, 4814, Australia

[4] CSIRO Agriculture, 306 Carmody Rd., St Lucia, QLD, 4067, Australia

[*] now at Murdoch University, 90 South St., Murdoch, WA, 6150, Murdoch, WA, Australia

[#] now at Faculty of Agriculture and Environment, Centre for Carbon, Water and Food, The University of Sydney, 380 Werombi Rd., Camden, NSW, 2570, Australia

Correspondence to: R. N. Handcock (R.Handcock@murdoch.edu.au)

Abstract

Timely and accurate monitoring of pasture biomass and ground cover is necessary in livestock production systems to ensure productive and sustainable management. Interest in the use of proximal sensors for monitoring pasture status in grazing systems has increased, since data can be returned in near real-time. Proximal sensors have the potential for deployment on large properties where remote sensing may not be suitable due to issues such as spatial scale or cloud cover. There are unresolved challenges in gathering reliable sensor data, and in calibrating raw sensor data to values, such as pasture biomass or vegetation ground cover, that allow meaningful interpretation of sensor data by livestock producers.

Our goal was to assess whether a combination of proximal sensors could be reliably deployed to monitor tropical pasture status in an operational beef production system, as a precursor to designing a full sensor deployment. We use this pilot project to 1) illustrate practical issues around sensor deployment, 2) develop the methods necessary for the quality control of the sensor data, and 3) assess the strength of the relationships between vegetation indices derived from the proximal sensors and field observations across the wet and dry seasons.

Proximal sensors were deployed at two sites in a tropical pasture on a beef production property near Townsville, Australia. Each site was monitored by a Skye SKR-four-band multispectral sensor (every 1 min.), a digital camera (every 30 min.), and a soil moisture sensor (every 1 min), each operated over 18 months. Raw data from each sensor was processed to calculate multispectral vegetation indices. The data capture from the digital cameras was more reliable than the multispectral sensors, which had up to 67% of data discarded after data cleaning and quality control for technical issues related to the sensor design, and environmental issues such as water incursion and insect infestations. We recommend having a system with both sensor types to aid in data interpretation and troubleshooting technical issues. Non-destructive observations of pasture characteristics, including above-ground standing biomass and fractional ground cover, were made every 2 weeks. This simplified data collection was designed for multiple years of sampling at the remote site, but had the disadvantage of high measurement uncertainty.

A bootstrapping method was used to explore the strength of the relationships between sensor and pasture observations. Due to the uncertainty in the field observations the relationships between sensor and field data are not conformational, and should be used only to inform the design of future work. We found the strongest relationships occurred during the wet season period of maximum pasture growth (January to April), with generally poor relationships outside of this period. Strong relationships were found with multispectral indices that were sensitive to the green and dry components of the vegetation, such as those containing the band in the lower shortwave infrared (SWIR) region of the electromagnetic spectrum. During the wet season the bias-adjusted bootstrap point estimate of the R^2 between above-ground biomass and the normalised ratio between the SWIR and red bands (NVI-SR) was 0.72 (95% CI of 0.28 to 0.98), while that for the percentage of green vegetation observed in three dimensions and a simple ratio between the near infrared and SWIR bands (RatioNS34) was 0.81 (95% CI of 0.53 to 1.00). Relationships between field data and the vegetation index derived from the digital camera images were generally weaker than from the multispectral sensor data, except for green vegetation observations in two and three dimensions.

Our successful pilot of multiple proximal sensors supports the design of future deployments in tropical pastures and their potential for operational use. The stringent rules we developed for data cleaning can be more broadly applied to other sensor projects to ensure quality data. Although

proximal sensors observe only a small area of the pasture, they deliver continual and timely pasture measurements to inform timely decision-making on-farm.

Keywords

Biomass, ground cover, calibration, wireless sensor network, beef production, extensive grazing, cattle, decision making, scale, multispectral sensors, digital cameras

1. Introduction

Frequent and accurate monitoring of pastures in livestock production systems is necessary to facilitate timely and appropriate management decisions. Traditional methods for measuring pasture biomass (e.g. pasture cuts, visual assessments and plate meters (Sanderson et al., 2001)) are time-consuming, leading to increased interest in automated monitoring methods. While remote sensing of the landscape from satellite-based platforms gives extensive spatial coverage, its usefulness can be limited by irregular availability of suitable images, which in tropical environments can be further restricted by cloud cover, particularly during the wet season when pastures are growing. Converting raw satellite images to a measure that is useful for on-farm decision making is also problematic due to the cost and processing requirements for operational delivery (e.g. Handcock et al., 2008). While cheap or free satellite images are increasingly accessible, their ability to be interpreted for decision-making on-farm is not straight forward. Continual monitoring using proximal sensors has the advantage over satellite images of capturing rapid-changes in the proportions of photosynthetically active vegetation (PV) (i.e. green) and non-photosynthetically active vegetation (NPV) (i.e. dead/dry). Such changes in the feed-base can signal that farm-management interventions are necessary for better utilization of resources and reducing detrimental environmental impacts due to overgrazing. For example, at the end of the wet season in tropical environments, beef producers need to assess how much green feed remains in the paddock to determine if there is sufficient feed to carry the herd through the dry season, or if they need to adjust stocking rates (O'Reagain et al., 2014), provide supplemental feed, or move animals.

With recent advances in wireless sensor networks and improved mobile network coverage, the delivery of monitoring data from sensors in remote cattle enterprises in a near real-time data stream has become feasible. While proximal sensors monitor only a small area or point and do not provide the extensive coverage of satellite imagery, when strategically placed within the farm, these sensors have the potential to deliver continual data on the feed-base and allow more responsive management decisions.

In the present study, proximal sensors refer to *in situ* sensors placed within several metres of the surface to be monitored, or placed in the shallow sub-surface environment, and providing repeat measurements at discrete intervals over periods of days to years. This distinguishes fixed proximal sensors from those which are mobile via robotic or aerial platforms (e.g. Von Bueren et al., 2015;Hamilton et al., 2007), vehicle-mounted sensors (e.g. King et al., 2010), or hand-held such as a field spectroradiometer (e.g. Peddle et al., 2001). While each of these moveable sensor types has their own advantages, such as covering large areas for the mobile sensors, or of targeted measurements in the case of hand-held sensors, none have the ability for easy long temporal coverage which is provided by fixed proximal sensors. Automated proximal sensors are of particular interest in extensive grazing enterprises in remote regions where access to repeat monitoring is costly and difficult, yet where remote sensing is not suitable due to issues such as scale or cloud cover.

There has been recent growth in the use of *in situ* proximal environmental sensors for a wide range of monitoring, including soils (Allen et al., 2007;Zerger et al., 2010), ecological studies (Collins et al., 2006;Hamilton et al., 2007;Szewczyk et al., 2004), temperate pastures (Zerger et al., 2010;Gobbett et al., 2013), forests (Eklundh et al., 2011), and sub-alpine grasslands (Sakowska et al., 2014), and to complement measurements made from flux towers (Balzarolo et al., 2011;Gamon, 2015). Networks to support the improvement of such sensors have recently been developed, such as through SpecNet (http://specnet.info), and the projects presented in the current special issue. Recent work on the use of digital cameras for repeat monitoring of vegetation includes using the camera images to estimate foliage cover in the forest understorey (Macfarlane and Ogden, 2012), forest phenology (Sonnentag et al., 2012), and gross primary production (GPP) of both forests and grassland and crops (Toomey et al., 2015).

Previous research using proximal sensing of pastures, aimed at assisting decision making in livestock production has employed handheld active multispectral sensors to measure green herbage mass and predict pasture growth rate (Trotter et al., 2010), plant height (Payero et al., 2004), nutrient composition using a handheld hyperspectral device (Pullanagari et al., 2012), pasture variability using multiple sensors (Serrano et al., 2016), forage biomass (Flynn et al., 2008), and forage quality (Zhao et al., 2007). While, these sensing devices can aid in farm decision making, such as grazing and livestock nutritional management, they are time consuming for the producer to implement, which reduces the frequency with which they are used. If proximal sensors were deployed permanently in pastures they could provide frequent information of temporal changes for timely management. These sensors may prove useful in livestock production under grazing conditions when decisions have to be made frequently (e.g. cell or rotational grazing) or at critical decision making periods such as during transitions between seasons

Converting sensor data to quantitative biophysical values, such as pasture biomass and groundcover, allows easier interpretation for making management decisions by livestock producers. Once calibration relationships are established, the data obtained from proximal sensors, such as spectral reflectance, can be related to biophysical values. An example is the well-established field of multispectral sensing using vegetation indices (e.g Tucker, 1979). Vegetation indices are frequently calibrated to the biophysical properties of the vegetation such as leaf area index (Turner et al., 1999), biomass (Pearson et al., 1976;Handcock et al., 2008), percentage vegetation cover (Lukina et al., 1999), or the fraction of photosynthetically active radiation absorbed by a canopy (Richardson et al., 2007;Myneni and Williams, 1994;Guerschman et al., 2009).

Our goal was to assess whether a combination of proximal sensors could be reliably deployed to monitor tropical pasture status in an operational beef production system, as a precursor to designing a full sensor deployment. We made a pilot deployment of sensors at two nodes located on tropical pastures in a beef production system. At each node a Skye SKR four-band multispectral sensor, a digital camera, and a soil moisture sensor operated over 18 months. The multispectral sensor data were calibrated using repeated visual observations of pasture characteristics supplemented by data from digital cameras, soil moisture sensors and weather data. We also developed methods for the management of multiple proximal sensors deployed in this environment and the quality control of such data, which extends on previous work in temperate pastures (Gobbett et al., 2013). We use this pilot deployment to illustrate:

1) practical issues around the sensor deployment,

2) methods necessary for the quality control of the sensor data, and

3) the strength of the relationships between vegetation indices derived from the proximal sensors and field observations of pasture status between the wet and dry seasons.

2. Methods

2.1. Field site and sensor nodes

The sensors were deployed at the Commonwealth Scientific and Industrial Research Organisation's (CSIRO) Lansdown Research Station, located 50 km south of Townsville, Queensland, Australia (19º 39' 42" S and 146º 51' 12" E, elevation 63 m). Paddocks used in this study contained pastures dominated by *Urochloa spp*., *Chloris spp.*, and *Stylosanthes spp*. Data were collected over 545 days between 23rd September 2011 and 21st March 2013.

Based on daily precipitation and temperature data collected by the Bureau of Meteorology (BoM) from the "Woolshed" station (approximately 45 km NW of the study site) the tropical climate in the study region is characterised by a wet season from November to April where monsoonal storms bring intermittent periods of heavy rainfall, and a winter dry season with little or no rainfall. The average annual rainfall of 1,139 mm falls mainly during the wet season, and the average monthly temperatures range is 20.8 to 28.5 °C in January, and 10.4 to 21.8 °C in July.

Each of the two sensor nodes (Figure 1were mounted with the same array of equipment (i.e. multispectral sensor, digital camera, soil moisture sensor, wireless networking infrastructure), and providing spatially-coincident data with both high temporal- and spatial-resolution. The nadir-pointing sensors were located at a height of 2.5 m above the ground. At this height the downward-pointing multispectral sensor had a 25° field of view (FOV) sensing approximately 0.97 m^2 of area at ground level, although this area changes across the season with vegetation height. The digital camera's FOV was approximately 2.8 m x 2.0 m at ground level, and would have been able to capture the 1 x 1 m area with a vegetation height up to approximately 1.5 m. See Balzarolo et al. (2011) for a discussion of optical sensor configurations.

The nodes were approximately 200 m apart in areas of the paddock visually assessed to be similar at the time of installation. One node was unfenced, permitting access to the area under the node by cattle grazing in the paddock. The second node was enclosed by a 30 m x 30 m fence, which excluded cattle from grazing within the enclosure, but allowed access by kangaroos and other small herbivores. The decision to place only one of the nodes within a grazing exclosure was made to improve the likelihood that the vegetation that was observed in each node would be at different heights. Although the paddocks were grazed by beef cattle for short periods during the sensor deployment, due to the lack of feed in the paddocks at those times and the low grazing pressures there ultimately was no discernible difference in vegetation height before and after the grazing.

Each node included a solar-powered sensor hub which relayed captured sensor data to a wireless sensor network (WSN) installed on the research farm, and via an internet connection to a centralized enterprise database. All equipment was temporarily removed for a week during a controlled property burn in mid-December 2011.

2.2. Soil moisture sensors

A Decagon "5TM" soil moisture sensor (Decagon Devices, USA) was installed at each node to monitor the volumetric water content (VWC) of the soil. The VWC is the volume of water per unit of total volume, determined by measuring the dielectric constant of the soil, as well as soil temperature from a thermistor. The 5TM sensors were buried at a depth of 15 cm under the soil surface below the multispectral sensors. This depth was used to capture soil moisture near the surface, yet reduce the possibility of damage from trampling by cattle. The 5TM sensors recorded soil moisture and soil temperature readings at 1 min intervals. We extracted an average of VMC for the period between 12:00 and 13:00 for each day, resulting in a time-series of daily VWC (i.e. SoilMoisture) and soil temperature data during the study period.

2.3. Weather data

The nearest BoM weather stations were at "Woolshed", "Charters Towers Airport" (both inland), and "Townsville Airport" (coastal), approximately 45 km NW, 70 km SW and 45 km N of the study site, respectively. Daily maximum ambient temperature averaged for the two inland stations had a strong relationship with temperature data from 12:00 from the 5TM soil moisture sensors, so these datasets were used interchangeably. The 5TM soil moisture sensors were additionally used as the main source of soil moisture data.

At the time of this study a new meteorological station at the Lansdown Research Station had recently been installed, but the data were not available for the study period. The national interpolated climate surfaces from BoM were thought to be too coarse for our small study site as precipitation events are typically spatial heterogeneous. Instead, a comparison of data from nearby BoM stations with the *in situ* soil moisture sensors at our nodes showed a strong correlation with the average of the precipitation recorded at "Charters Towers Airport" and "Townsville Airport" stations (Pearson product-moment correlation coefficient of 0.61 during the wet season period of data collection).This average precipitation was therefore used as the best option, as the only alternative was to use an interpolated dataset.

The start and end of the wet season was determined using a method designed for the North Australian climate (Lo et al., 2007) in which the start of the wet season is defined as the date after 1st September when 50 mm of precipitation has accumulated. Bureau of Meteorology precipitation data from the "Townsville Airport" station were used to define the start and end of the wet and dry seasons, as this station had the most complete time-series of the nearby stations.

Using this method, the 2011/2012 wet season at our study site started on the 5th December 2011, and the 2012/2013 wet season started on 1st January 2013.

2.4. Digital Cameras and the VegMeasure semi-automated classification

Digital cameras were deployed at the study site to provide an automated assessment of ground cover (see Zerger et al., 2012), to serve as a visual cross-check of the multispectral data, and to assist in identifying surface water. At each of the two nodes we deployed a Pentax Optio WG-1 digital camera in a downward-pointing position, centred on the area sensed by the Skye sensors so that the images overlapped the FOV of the multispectral sensors.

This camera model was selected as it was inexpensive, weatherproof and had an inbuilt intervalometer to enable automatic shooting at fixed intervals. At 2.5 m the 13.8 megapixel digital cameras recorded images with an approximate resolution of 0.6 mm at the ground. The cameras were configured with flash off, sensitivity at ISO 200, autofocus and automatic white balance enabled. The decision to use an automatic white balance was based on similar studies (e.g. Macfarlane and Ogden, 2012), although other studies have used a manual/fixed white balance in order to minimize changes in illumination (e.g. Toomey et al., 2015;Sonnentag et al., 2012). Digital images (approximately 1 to 4 MB each) were captured every 30 mins and were manually downloaded at approximately 2-week intervals.

The images from the cameras contained uncalibrated red, green and blue (RGB) spectral bands. There has been extensive work on automated and semi-automated classification of such time-series of digital photographs for the purposes of vegetation monitoring (e.g. Ewing and Horton, 1999;Karcher and Richardson, 2005;Bennett et al., 2000). As the focus of the current study was on the calibration of the multispectral sensor data, we chose to use a semi-automated method, VegMeasure (Johnson et al., 2003), to extract a green cover fraction from the time-series of digital camera images at each node. VegMeasure has been utilized and validated in a number of studies (e.g Booth et al., 2005;Louhaichi et al., 2001) and provides a rapid method to classify a series of images into green and non-green using the Green Leaf Algorithm (GLA). The GLA also acts as an alternative sensor measurement of green fraction to that derived from the multispectral dataset.

The GLA protocol requires deriving a single threshold value from a single image which is then applied across the whole time-series of camera images. The GLA applies the following spectral band ratio (Louhaichi et al., 2001):

$$\frac{(G-R)+(G-B)}{(\mathrm{G}+\mathrm{R}+\mathrm{G}+\mathrm{B})}. \quad (1)$$

where G is the digital number of the green band, R is the digital number of the red band and B is the digital number of the blue band. The proportion of the pixels in each image in which the band ratio exceeds a user defined threshold, is reported as the GLA.

For each day in the study period, the camera image taken nearest in time to 12:00 was selected to minimise shadows and to ensure as consistent illumination as possible, and the time-series was quality controlled for days when there was site maintenance work under the node. One photo with a mix of PV (i.e. green) and NPV vegetation was manually selected as a calibration image (14 May 2012, 12:13:55 GMT, on the unfenced node). To derive a threshold value for the GLA, one hundred random points were identified using the "Calibrate threshold" function in the VegMeasure software , and assigned to two classes: "white" = green vegetation and "black" = non-green vegetation and background material including litter and soil). The resulting GLA threshold of 0.095 was verified using a random selection of images and was then applied across the whole time-series of camera images to extract the green proportion. The single threshold value used in deriving the GLA is a necessary feature of using the GLA, as well as having been applied in other vegetation studies (as cited).

2.5. Multispectral sensors

We used a paired sensor setup (Figure 1) with the downward-pointing sensor having a conical field of FOV of 25° as indicated by the manufacturer, allowing it to sense reflected light only from the ground directly beneath the sensor. The upward-pointing sensor was fitted with a cosine diffusing filter to alter its FOV to a full hemispherical view, permitting the albedo of the surface to be assessed relative to the incident solar radiation. Sensors were checked and cleaned fortnightly and the sensor station coated with insecticide to deter crawling and flying insects.

The multispectral sensors mounted on each of the two nodes were paired Skye SKR-1850 four-band weatherproof sensors (Skye-Instruments, 2012b), which were calibrated individually by Skye, with band choices based on our specifications. Each sensor was configured with bands in the green (0.545 to 0.547 µm), red (0.644 to 0.646 µm), near infrared (NIR) (0.834 to 0.837 µm) and the lower SWIR (1.028 to 1.029 µm) spectral range (wavelengths in brackets indicate band widths). These bands were chosen as the NIR region of the electromagnetic spectrum is widely used in monitoring vegetation 'greenness' from multispectral sensors (Tucker, 1979), and the SWIR region is sensitive to plant moisture content (Tucker, 1980). Both the SWIR and upper

NIR spectral data can be used to help differentiate PV from both NPV and soil (Asner, 1998), and broad-band SWIR indices have been used to capture seasonally-varying NPV proportions resulting from repeat grazing of pastures by livestock (Handcock et al., 2008). We were not able to choose the fourth sensor to be in the 1.55–1.75 µm range recommended by (Tucker, 1980), but were limited to using the longest wavelength possible for this sensor configuration to try and capture senescing vegetation. The band choice was verified before sensor creation by comparing the band to reflectance for green and dry pastures from the ASTER spectral library (Baldridge et al., 2009). This comparison confirmed that, while the discrimination between green and dry pastures is not as distinct at 1.029 µm compared to that at 1.55–1.75 µm, there was still enough potential for discrimination to confirm this wavelength choice for the fourth band.

2.6. Vegetation indices

The NIR region is sensitive to vegetation "vigour" or "greenness", and vegetation indices, such as the widely used normalized difference vegetation index (NDVI) (Tucker, 1979) utilize the NIR spectral range. A variety of vegetation indices are possible from combinations of the four broad spectral bands of our Skye sensors. Due to the algebraic complexity of calculating indices from this particular Skye sensor model (see the description in the paragraph below), our index choice was limited to simple ratios and normalized difference band ratios (Jackson and Huete, 1991), which we derived to highlight seasonal aspects of the green and dry mix of the tropical pastures (Table 1).

The Skye sensors returned a calibrated numeric output for each spectral band every minute, and data volumes were small enough to be transmitted in near real-time via the WSN. After calibrating raw sensor data using individual Skye sensor calibration coefficients, vegetation indices were calculated. The Skye SKR-1850 sensor does not permit the calculation of reflectance directly from the raw current. Instead, Skye provides formulae which use the measured sensitivities of the individual sensors to calculate ratio-style indices such as NDVI (Skye-Instruments, 2012a). These indices are mathematically equivalent to those calculated from reflectance. Using the NDVI example from Skye, we developed formulae for the vegetation indices shown in Table 1.

2.7. Quality control of the sensor data

We illustrate the types of processing required for high-frequency multispectral time-series with an example of a typical diurnal time-series of multispectral data with a reading every minute (

Figure 2). Both raw sensor current and the calculated NDVI values are typically low during the night-time hours. The period of rapidly increasing sensor values at dawn is extremely noisy due to variable early morning illumination and the scattering of sunlight through a thicker atmosphere at low elevations. At dusk this pattern of sensor values is reversed (data not shown), which is also seen in Weber et al. (2008: Figure 3a). Apart from the spike in high NDVI when a green leaf was held in front of the sensor (approximately 13:00), the middle part of the day is the period of relatively stable values of NDVI, with only random variations that occur due to the noise in the raw current, or from ephemeral variations in illumination such as from sun glint.

For the entire time-series of multispectral sensor data taken every minute, a time-series of daily values was determined by selecting the vegetation index values from the middle part of the day (12:00 to 13:00) and calculating the median value to reduce noise due to small fluctuations in illumination. Data from a particular day were discarded if they met any of the four categories of filtering criteria listed in Table 2. Data were not discarded under conditions where changes in the spectral values were considered to be a signal rather than noise. For example, rapid increases in NDVI values over time corresponded to rapid growth at the start of the wet season, and so were not filtered. Questionable multispectral data were also visually verified against the digital camera images. In developing these filtering rules, the vegetation indices stood as proxy for their individual constituent bands since, as discussed, it was not possible to use spectral reflectance from the Skye SKR-1850 sensors directly. Table 2 is divided into four different filtering categories as follows.

The first category of filtering criteria (Table 2a) were developed to screen the daily multispectral data series for large fluctuations such as data outliers, spikes, high noise levels, data out of range, clipping and calibration issues, which can commonly result from anomalies at the sensor or during data transmission (Collins et al., 2006;Ni et al., 2009). For example, the night-time raw current reading should remain relatively constant, excluding minor night-time light reflections or electronic noise. Large deviations from night-time baseline current values indicate a technical issue. Such issues were identified from the night-time (00:00 to 01:00) median value of raw current by flagging where one or more of the multispectral sensor bands in the paired node had a night-time reading greater than 10,000 mV, or where these values were greater than 3 standard deviations from the band mean value. The day-time (12:00 to 13:00) median value of the multispectral indices was also used to identify data quality issues, for example where NDVI was not between 0 and 0.1. This threshold value of NDVI was chosen based on typical values for this environment (Holben, 1986;Jackson and Huete, 1991), and would have to be adjusted if the sensors were deployed elsewhere, for example to monitor snow and ice which may have negative NDVI values. Data were also masked when the daytime RatioNS34 dropped to zero but within one day had returned to its previous value. All instances where the RatioNS34 remained at zero for more than one day were visually cross-checked with the deployment records to see if this indicated sensor failure or some other issue such as an insect infestation.

The second category of filtering criteria (Table 2b) is for logistical and physical issues. For example, the data for a day was screened if there was a maintenance ladder underneath the sensor. Or when a sensor was swapped for new equipment, this required that a new baseline current value be used in calculations that use raw current. A flag was also set to indicate days where there was no data during the midday period from one or more of the sensors, which would restrict the calculation of a full suite of indices.

The third category of filtering criteria (see Table 2c) covers filtering rules based on the expected spectral response of tropical pastures. For example, if NDVI was less than zero. This flag is a companion test to the range tested in Table 2a, as it flags NDVI ranges that may indicate catastrophic failure of the sensor resulting in values extremely out of range. All of these cases were visually examined through the photographs and by inspecting the sensor infrastructure during site visits. Other indices were also used for testing data out of range. For example, if RatioNS34 values were greater than 2, this indicated a technical error as pastures should not have values in this range. This filtering rule would need to be adjusted if the sensors were deployed to a different environment. When values of gNDVI were less than 0 or values of NVI-GR were greater than -0.10, and the date and weather data indicated that the readings were made in the dry season, this again indicated values that were out of range rather than due to wet season surface water.

The fourth category of filtering criteria (Table 2d) covered filtering rules where valid spectral signals were excluded, not because they were errors, but because they covered physical conditions which were not applicable to our goal of monitoring pastures. For example, surface water under the vegetation due to heavy rainfall was identified by visual inspection of the camera images combined with the soil moisture data, and filtered because it was not a valid measurement of the pasture status even though it was a valid sensor signal.

2.8. Field observations of vegetation made under the sensor nodes

In designing the field sampling for this project it was necessary to balance the project goals with staff resources and logistics of travelling to the remote site every 2-3 weeks for the multiple years of the sensor deployment. All field observation methods were designed to be quickly completed by field technicians during these visits, while also maintaining the technical infrastructure of the sensor deployment. This trade-off between time and resources (Catchpole and Wheeler, 1992) resulted in field observations successfully being obtained over the multiple years of the study, but also resulted in a large degree of uncertainty in the field observations.

During the study period there were 32 visits to the study site to make field observations. All the measurements were made by the same two field technicians, with the majority (71%) by one technician. Where possible, measurements were repeated by both of the main technicians or other staff (6 days). For the 45% of days where more than one technician made measurements, the data from that day was averaged. Visual examination of the raw field data noted no systematic differences between the data collected by the different field technicians, so measurements were not further controlled for operator differences. All observations were made within the sensors FOV in a 1 m x 1 m area under the sensors identified by small pegs hidden by the vegetation.

Pasture Biomass

In temperate pastures, biomass is commonly measured using destructive sampling, with the vegetation cut from a sample quadrat being dried and weighed (Catchpole and Wheeler, 1992). For pastures where the spatial variability is high, such as at our study site, destructive sampling is also not recommended (Tothill, 1998) because of the difficultly in making biomass cuts in dense vegetation. Destructive sampling of the area under the sensors was also not desirable as this would have restricted the range of pasture biomass measurements to only low values, and the pastures would not re-grow rapidly enough for accurate visual assessment of biomass if they were cut to ground level. An alternative approach of destructive sampling at nearby locations was also not suitable as the tropical pastures are naturally heterogeneous at the local scale, and the area around the sensors will be highly variable in both biomass and species composition. We therefore limited sampling to the FOV of the multispectral sensors.

An alternative to destructive sampling for assessing pasture biomass in tropical pastures is the non-destructive BOTANAL dry-weight ranking method (t'Mannetje and Haydock, 1963;Friedel et al., 1988) which can be used to estimate pasture composition as well as the pasture yield

(Tothill et al., 1992;Orchard et al., 2000). A key technique in the BOTANAL method is that visual estimates are verified against pasture cuts from which a calibration relationship is developed. However, the BOTANAL assessment was determined as being too time consuming for the long duration of the pilot study, and we instead developed a less time-intensive set of field observations, which are described below.

For our quick field assessment of above-ground standing biomass (weight of above-ground vegetation dry matter (DM) per unit of area, (kg DM ha^{-1}) we used non-destructive visual assessment within the sensor FOV to pasture photo standards (Queensland Department of Primary Industries, 2003). These pasture photo standards were developed as the industry standard for beef producers to assess pasture status (Department of Resources Northern Territory Australia and Meat and Livestock Australia, 2012). For field observations of above-ground standing biomass (called TotalBiomass henceforth) which were less than 3,000 kg DM ha^{-1} the predominant pasture photo standards used were those for a mixed pasture of "Eucalyptus Box" and "Stylo", with the group "Eucalyptus Box" used for pastures above 3,000 kg DM ha^{-1}. Where the vegetation was clearly between two photo standards the observation was visually interpolated (Queensland Department of Primary Industries, 2003)

For days where we had a second field technician repeat the observation, the average difference between the two observations of TotalBiomass was 570 kg DM ha^{-1}, but ranged from zero to as much as 2,400 kg DM ha^{-1}. When these operator differences are combined with the wide spacing of biomass in the reference photographs, as well as any additional uncertainty introduced by the visual nature of the assessment, the total uncertainty in the TotalBiomass is high and must be used with caution. Recommendations for alternative sampling methods for future work will be made in the discussion section.

Fractional Cover

The mix of PV and NPV in the vegetation is an important factor in monitoring pasture changes over time. TotalBiomass was not divided into PV (i.e. green) and NPV (i.e. %dead/dry) biomass components as the pasture reference photographs used for assessing these tropical pastures are not suitable for such an application. We instead made visual assessments of fractional cover measurements as a way of capturing the PV and NPV components of the pastures. The fraction of bare ground and the fractional coverage by PV and of NPV are widely used for assessing landscape degradation (Richardson et al., 2007;Myneni and Williams, 1994;Guerschman et al., 2009), although for a non-expert in remote sensing the fractional cover is a less familiar measurement than TotalBiomass to interpret and use.

The visual field assessments of fractional coverage were made in two dimensions from above, across a 1 m by 1 m area under the sensor's FOV as follows:

$$\%TotalVegetation2D + \%BareGround + \%Litter2D = 100\% \quad (2)$$

where %BareGround is the percentage bare ground as seen in 2D, %Litter2D is the percentage of litter which is not attached to any plant, and TotalVegetation2D% is the percentage of vegetation still attached to the plant, including both green (PV) and dry (NPV) vegetation as both typically remain on the plant during at least the early dry season. We also visually assessed the percentage of just the visible green proportion of the vegetation, as seen in both two dimensions, looking down at the plot (%Green2D), and three dimensions, looking at the whole plants within the plot (%Green3D). While not as useful as actual measurements of green biomass, these 2D and 3D visual assessments give the nearest approximation of green vegetation without destructive samplings and separating green and dry material. For days where we had a second field technician repeat the observation, the average difference between the two observations of %BareGround was 11% (range 1-35%), of %Litter2D was 6% (range 0-30%), of %Green3D was 12% (range 0-50%), and of %Green2D was 5% (range 0-30%).

Vegetation Height

The 1 m x 1 m area under the sensor FOV was divided into four quadrants and vegetation height (VegetationHeight, cm) was measured using a ruler for each quadrant. Vegetation height was also measured across the sampling area as a whole, by assessing the height at which 95% of the vegetation was below. The final VegetationHeight value was the average of the five measurements.

2.9. The relationship between sensor and field data

The goal of this part of the project was to assess whether the sensors were able to deliver a reliable source of data that can be calibrated to biophysical values. Our goal was not to develop definitive relationships for prediction purposes, as the quality and volume of the field data is not sufficient for that purpose. We instead assess only the strength of the relationship between the sensor and field data, and do this separately for data from the wet and dry seasons and across the whole year. We use these results to recommend when and how data should be collected in a full sensor deployment for monitoring on-farm.

Data from the two nodes were combined as there were no discernible differences between the fenced and unfenced samples due to grazing of the pastures by cattle. Of the original 33 days of field measurements from across the whole project, Table 3a shows the number of days where the field sampled data matched the filtered sensor data at each node. Data subsets were also created for the wet season period from January to April (days 1 to 130 of the year), and the dry season (May through December) (Table 3b). The remainder of the field samples were made during periods where the sensor data were filtered using the rules in Table 2 and so could not be used for further analysis.

The final group of independent variables included vegetation indices derived from the filtered daily dataset from the multispectral sensors (i.e. NDVI, gNDVI, NVI-GR, NVI-SR, and RatioNS34) and the digital cameras (i.e. GLA). The dependent variables were the visual biophysical measurements and other observations of the pasture status made at the field sites (TotalBiomass, %BareGround, %Litter2D, %TotalVegetation2D, %Green2D, %Green3D, and VegetationHeight).

2.10. Model development

A common problem in calibrating and validating models between remote sensing and field data is the small number of field samples and the inherent variability in biophysical data, resulting in models that are not robust (Richter et al., 2012;Harrell et al., 1996). Richter and others (2012) provide a good overview of statistical techniques useful for such datasets, including the use of cross-validation and bootstrapping methods for model development and validation. Bootstrapping is a non-parametric method that does not assume normality of the dataset, making it suitable for developing robust estimates of the population from limited sample data such as in the present study. The estimated model coefficients are assumed to be the best estimates of the population values (Harrell et al., 1996), of which our field observations are just one sample of the entire population. The advantage of the bootstrapping method is that the entire dataset can be used to assess the model performance in the one process, rather than having to split it to create a validation subsample (Harrell et al., 1996). The distribution of model parameters resulting from the bootstrapping allows the confidence intervals and standard errors of the model parameters to be estimated (Peters and Freedman, 1984).

In the bootstrapping method, a sample is drawn from the original dataset with replacement, meaning that each individual datum is selected from the whole dataset and so could be drawn multiple times. For each sample, the desired model is fitted between the dependent and independent variables, and their model coefficients are determined. The sampling and modelling process is repeated many times, with 200 being the minimum recommended by (Steyerberg et al., 2001). The result is a distribution of the selected model parameters from which the robust estimates of the model parameters and confidence intervals can be made.

The bootstrapping approach is particularly suited to our pilot study because we are interested in the strength of the relationships between the sensor data rather than their form. The approach also addresses the main issue with the visual assessment of pasture status, which is the high degree of uncertainty in that data. The bootstrap method replicates all uncertainty in the analysis, including operator error, uncertainty in the field observations, and that from the flexibility of the statistical model, allowing the confidence intervals around the model parameters to be assessed (Carpenter, 1998). The method is robust in cases where one variable has missing data, such as where the filtering of our spectral data resulted in field data which did not have matching sensor data.

We therefore applied a bootstrapping method to assess the strength of the relationship between the sensor and field data and the uncertainty around the model parameters. All analysis was made using the R statistical package (R-Core-Team, 2013). We used the "*mgcv*" library in R (Wood, 2011) to fit generalised additive models (GAM) (Hastie and Tibshirani, 1990) with a maximum possible dimension of four. GAMs do not assume a linear relationship, but instead use a non-parametric method to fit a model with the highest dimension possible given constraints of small datasets and missing data. The bootstrap was implemented using the "*boots*" library in R (Carpenter, 1998) with 2,000 model runs and a "Pivotal" method. This bootstrapping method was applied to all combinations of observations of pasture status, and a single independent sensor variable.

3. Results

3.1. Multispectral sensor data

As the multispectral measurements were made every minute, the data collection from the two nodes represents a possible 1,569,600 sets of the eight raw current values. As a result of the rigorous data cleaning using the criteria in Table 2, for the 545 days of data collected at each node, 48% of days of data from the unfenced node and 63% of days of data from the fenced node were discarded. This large number of filtered days of data reflects the experimental nature of the pilot deployment of the sensors, which resulted in technical and environmental issues with the sensor deployment. However, the rigorous data cleaning we applied was necessary to ensure quality data for model development.

Figure 3 illustrates this data cleaning by showing the time-series of NDVI values from the unfenced node, before (raw) and after filtering. In comparison to the digital cameras, the design of the housing for the Skye SKR-1850 sensors led to significant problems with insects such as mud-wasps nesting in the sensor tubes (Figure 4 a-b), spiders building webs across the sensor openings, and water ingress below the cosine correction filters which were fitted to the upward-pointing sensors.

3.2. Field observations

The field observations made at each of the two nodes (Figure 5) illustrate the rapid vegetation growth at the start of the wet season followed by senescence during the dry season. During the 2011-12 wet season the TotalBiomass observed at the two nodes had similar values (Figure 5a), despite the recognised uncertainty in these measurements. Having initially similar pasture biomass was not unexpected as the nodes were sited in an area of the paddock with similar vegetation. Although we had fenced one node with the intention of increasing the range of pasture height being monitored, due to the limited feed availability in the paddocks and the low grazing pressure, these grazing events had negligible impact on the pastures and were not considered further in the analysis.At the end of the 2011-12 wet season the TotalBiomass observed at each node became markedly dissimilar, with differences of almost 2,000 kg DM ha^{-1} between the nodes, and as expected the difference continues during the rest of dry season as there is no rain to promote vegetation growth. This difference in the pasture biomass between the nodes illustrates the heterogeneous nature of these pastures, where a small change in the type, size, shape, and density of the vegetation growing under a node resulted in large biomass differences. It also highlights why pasture measurement made in the area surrounding the node may not be representative of what the sensor FOV observes.

The time-series of VegetationHeight (Figure 5b) shows a similar pattern to TotalBiomass, but the differences between the nodes are less distinct. VegetationHeight also exhibits more variability between measurements despite being a quantitative measurement made with a ruler rather than a visual estimate. In contrast, the observations of %Green2D, and %Green3D (Figure 5c and d) are comparatively similar between the two nodes, except for the period of June to July 2012. As shown in the images in Figure 6, the vegetation is tall, mixed, senesced, and increasingly lodged (i.e. no longer erect), resulting in increased variation in the observed values between the nodes.

3.3. Time-series of digital camera images and GLA

Over the 545 day study period, the digital cameras captured 22,642 images at the unfenced node and 23,210 from the fenced node. Data capture from the cameras was more reliable than for the multispectral sensors with the loss of only 13 days of data from the unfenced node (3%), and 10 days of data from the fenced node (2%), both due to data card failure. A month of digital camera images was also lost in a post-capture storage malfunction, so is not counted as being a deployment-related data loss.

Figure 6 shows a time-series of images from the digital camera at the fenced node, with each week represented by one image taken at approximately 12:00. The seasonal progression of vegetation is clearly illustrated by these images, from the new green growth of the vegetation at the start of the wet season, followed by senescence during the move into the dry season, and the sudden removal of all vegetation following the 2011 controlled burn. The camera images again illustrate how, as the wet season progresses, the tall grasses dominate the canopy followed by the gradual drying of the canopy in the transition into the dry season.

Figure 7 shows the daily time-series of GLA calculated from digital camera images at each node. These results show that the digital cameras and GLA can successfully capture the seasonal changes in green vegetation, corresponding with the rapid growth of green vegetation at the start of the wet season followed by a decrease to zero during the dry season.

3.4. The relationship between sensor data and field observations

Table 4 and Figure 8 show the bias-adjusted bootstrap point estimates, and the lower and upper bound of the 95% pivotal bootstrap confidence intervals, for the distributions of R^2. These distributions are from bootstrapping the GAMs for all combinations of sensor-derived indices and field observations, which were made of all data, as well as for the data subsets from the wet or dry seasons. As the bias-adjusted bootstrap point estimates of R^2 are a more conservative estimate than the mean R^2 of the modelled distribution, there are times when its value is negative, or less than the lower bound of the 95% pivotal bootstrap confidence interval. This occurred most frequently for the dry season data where the model fits are generally poor (Table 4). The graphs in Figure 8 clearly show how the various uncertainties in the study, and in particular the high uncertainty in the field observations, has resulted in wide confidence intervals for many of the models explored using the bootstrapping methodology.

The relationships between sensor and field observations for the whole year and dry season period generally performed poorly compared to those from the wet season. These results are not unexpected as the vegetation between the wet and dry season in this environment is distinctly different. The exceptions were for %Green3D (Figure 8e) and %Green2D (Figure 8f), which for all sensor-derived indices except RatioNS34 had strong relationships to data from the whole year and dry season. The bootstrapping analysis for %Green.2D was not able to determine model parameters due to the boundary conditions inherent in those subsets of data values.

Across all time periods, the strongest relationships between the multispectral sensor and pasture observations were for the wet season data for %Green3D (Figure 8e) and %Green2D (Figure 8f). For all variables, %Litter2D (Figure 8c) showed the weakest relationships with the sensor variables, and %TotalVegetation2D (Figure 8d) showed only weak relationships. For the other pasture observations there were good relationships with at least one sensor variable. For example, the bias-adjusted bootstrap point estimates of R^2 for the wet season data between TotalBiomass and NVI-SR were 0.72 (95% CI of 0.28 to 0.98) (Figure 8a), %BareGround and gNDVI were 0.65 (95% CI of 0.09 to 0.92) (Figure 8b), %Green3D and RatioNS34 were 0.81 (95% CI of 0.53 to 1.00) (Figure 8e), and VegetationHeight and NVI-SR were 0.66 (95% CI of 0.19 to 0.95) (Figure 8g). Excluding the relationships for %Litter2D, for four of the other pasture observations, the NVI-SR index had the strongest relationships to four different pasture characteristics, with RatioNS34 for one variable (%Green3D, Figure 8e), and gNDVI for one variable (%BareGround, Figure 8b).

Across almost all time periods, the relationship between the image-derived GLA were weaker than those from the multispectral sensor data. The one example where the GLA outperformed the multispectral sensors was also the strongest relationship in all data and periods, being for data from the whole year, and between %Green3D (Figure 8e) and %Green2D (Figure 8f). These results show that the GLA method to extract green fractions from the digital camera images was very successful in this environment.

4. Discussion

The tropical pasture conditions in the present study presented unique technical issues that had to be overcome as part of the deployment of proximal sensors, including marked wet and dry seasons, high humidity, rapidly growing vegetation, fire and insects.

4.1. Assessing pasture status

In this study, the time-series of images from the digital cameras and multispectral sensors at each node clearly captured the changes in the tropical pastures; from the period of green-up at the start of the wet season, the period of green vegetation growth during the wet season and the gradual senescence and drying off of the vegetation. Even given the obvious limitations with the observations of pasture status in this study, it is clear that there are stronger relationships during the wet season than during the dry season or for the whole year. The generally poor relationships between the sensor and field observations outside of the wet season are not surprising since NPV is difficult to discern in the NIR spectral region. The SWIR band of our multispectral sensors was also in the lower part of the SWIR range (1.029 µm), which is not as responsive to dry vegetation as the longer SWIR region of the visible to near-infrared (i.e. 1.55–1.75 µm) that (Tucker, 1980) recommends for the remote sensing of plant canopy water status. Even if the issues with the field data quality are overcome in a future deployment, it is unlikely that the relationships between field and sensor data will improve for the dry season unless the choice of spectral bands in a future deployment was made to improve sensitively to NPV.

4.2. Fractional cover

The results of using the bootstrapping method to explore the relationship between the pasture observations shows that the various measures of fractional cover could be successfully predicted from various indices calculated from either the multispectral sensors or the digital camera data. These results are encouraging for additional studies exploring these relationships further.

These results also showed the GLA derived from the digital images to be a useful parameter, with strong relationships to the field observations of %Green3D and %Green2D. They also support the utility of including a SWIR band in the multispectral sensors, with data from our multispectral band in the lower SWIR giving encouraging results.

The vegetation indices from the multispectral sensors were a better predictor of %BareGround than the GLA from the digital cameras. These results indicate that while both sensor types are suitable for monitoring aspects of fractional cover in this tropical pasture system, alternative indices extracted from the digital cameras would need to be explored to improve how well

%BareGround can be monitored. Both sensors view the canopy in two dimensions, with the GLA focussed on the green proportion of the canopy while the band choice for multispectral indices can be made to capture both PV and NPV.

Fractional cover has the potential to be a valuable part of a multiple data source approach to providing on-farm data to farmers for sustainable pasture management. Although fractional cover is widely used in landscape degradation studies, particularly in regional monitoring (Richardson et al., 2007;Myneni and Williams, 1994;Guerschman et al., 2009), it is a more recent measurement compared to pasture biomass which has long been used in livestock production systems. Fractional cover is therefore a less familiar measurement than biomass to interpret and use. However, as fractional cover measurements become more widely available (e.g. Guerschman et al., 2009) and examples of its use in operational farm management increase, it is likely that this will change, as occurred when NDVI started to be used in agriculture. Sensor nodes that monitored fractional cover could be strategically placed in sensitive areas to monitor areas that are becoming over-grazed, for example to signal an alert to move livestock.

4.3. Data interpretation at different times of the year

Although the period at the end of the wet season is critical for on-farm decision making, we recommend that to improve understanding of the rate of change of the pasture conditions, monitoring also be made throughout the wet season that precedes it and into the start of the dry season. One of the benefits of a data flow from proximal sensors is to understand the rate of seasonal changes, and identify any periods where the pasture conditions change rapidly or suddenly in response to weather or environmental events.

From this pilot project it is still unclear whether pasture biomass could be predicted with sufficient accuracy in this environment to allow the measurements to be used operationally in decision making on-farm. However, the results of the present study are encouraging enough to show that further work is warranted. Assuming that the issues with the field data quality can be addressed in future work, it is expected that the relationships between field and sensor data will improve.

This study was run for less than two years, and covers only the limited range of pasture conditions resulting from inter-annual variability in climate and differing grazing and pasture management. If further studies do not show consistent relationships between sites and years, one option for calibration would be to have the farmer performing a controlled set of calibration measurements once or twice during the growing season to calibrate a particular sensor deployment. Having to make pasture measurements would require additional time from labour-poor beef producers. However, by gathering this data at the geographical location of the deployed sensors, these measurements would alleviate the cost of a much larger project. This larger project would require gathering the volume of calibration data required to develop models that would be robust for different geographical locations and different weather conditions between years, and address any re-calibration requirements of the physical sensor over time. Alternatively, the time-series of vegetation index data from the sensors could be used without calibration to a quantitative value, which would still provide data to indicate sudden changes in vegetation growth.

4.4. Accuracy of the field data

It is clear that the accuracy of field observations of pasture status could be improved for future sensor deployments aimed at developing qualitative relationships between sensor and field data. In the context of the present study, the uncertainty in our field observations does not change the main outcomes of the project, which are to illustrate practical issues around the sensor deployment, and the methods necessary for the quality control of the sensor data, necessary for designing future deployments.

We recommend that future deployments use non-destructive sampling methods such as BOTANAL, which includes a protocol for assessing and maintaining the accuracy of visual measurements of pasture biomass and composition (Tothill et al., 1992;Orchard et al., 2000). Alternatively, visual assessments could be calibrated by developing a site-specific set of reference photographs at different times in the growing season. The reference photos would be calibrated using pasture cuts (if possible for the vegetation type), and used for repeat training of field staff. This method has the advantage of controlling the data range and the biomass interval between photo standards. Pasture assessments of this type are time-intensive, which could be mitigated by targeting data collections at key times during the year. It would also be useful to make additional measurements in the vicinity of the node FOV to assess the spatial variability of pastures in the surrounding area.

4.5. Data filtering

In the extensive database cleaning illustrated in Figure 3 and Table 2 we focused on post collection filtering methods, as the experimental nature of our deployment meant that data could not be screened in real-time. In an operational system additional rules and approaches could be implemented on the node, such as for sensor data cleaning and outlier detection (e.g. Basu and Meckesheimer, 2007;Huemmrich et al., 1999;Liu et al., 2004), and including implementing data quality control algorithms within the WSN (e.g. Collins et al., 2006;Jeffery et al., 2006;Zhang et al., 2010). In addition to the data cleaning rules we developed, and as the field deployment progressed, we modified the sensor maintenance protocols and infrastructure. This knowledge can also be used in future deployments.

Due to our stringent data cleaning protocols, a large amount of data from the multispectral sensors was excluded by a combination of automatic and manual methods. In future deployments additional automatic data filtering could be implemented, for example using spectral information to filter data when surface water is present. Developing automatic filtering rules for surface water was not considered necessary in our study as visual examination of the digital camera images identified only 9 days of surface water at the fenced node and 20 days at the unfenced node. The data were excluded manually, particularly as this surface water occurred when there was water incursion into the sensor housing and the whole data period was suspect. For sensor deployments in conditions with more surface water, such as in areas of flood irrigation, having an automatic rule for surface water detection would be useful.

4.6. Comparing camera and multispectral sensors

We found the digital cameras to be more robust than the multispectral sensors in terms of data flow, with up to 63% of days of data from our Skye sensors being discarded during data quality control. Although the stringent filter criteria (Table 2) may have resulted in some “clean” data being excluded, this was balanced against the greater impact of having untrustworthy data for modelling. The long periods of erroneous multispectral data showed this Skye SKR-1850 sensor model was unreliable in the environment. In comparison to the digital camera, the design of the Skye sensors led to significant problems, including insect infestations in the sensor tubes, and water ingress below the cosine correction filters which were fitted to the upward-pointing sensors.

While we were able to mitigate the effects of these issues by regular maintenance of the sensors and post-acquisition data cleaning, we found that the Skye SKR-1850 sensor model was not stable enough in our tropical environment for an operational deployment on a farm. For example, we had the complete failure of one sensor which had water incursion into the sensor enclosure at the point where the wiring attached to the sensor, despite sealant being applied to the connection and the connections being regularly monitored. Given that we had a spare sensor that could be used as a replacement, the decision was made to swap the sensors out to ensure continuity of data collection while the sensor was returned to the manufacturer for examination.

The new and improved designs for the Skye sensor housing are likely to address many of these issues by having a covered sensor face and also being able to calculate reflectance directly (e.g. the SKR 1860D 4 channel sensor design Skye-Instruments (2013). Repeating this study with the newer sensor design would allow the focus of future studies to be on gathering multispectral measurements, not on checking and managing the technical aspects of the field deployment, or on post collection data filtering. In situations where only the earlier model Skye sensors are available for use, it may be possible to use a method employed byHarris et al. (2014) who were able to overcome similar limitations of earlier models of a SKR-1800 sensor by using a cross-calibration method between the upward- and downward-pointing sensors to retrieve reflectance. While not recommended by the manufacturer, such a method would be useful for deployments where the calibration certificates had expired, or where reflectance is a requirement.

Cross calibration of sensors could also be useful in situations where there is a mix of sensor types deployed to capture spatial variability in the landscape. The growing availability of lower cost sensors provides an alternative to expensive but highly calibrated sensors such as the Skye SKR-1850, with arrays of lower cost sensors relying on multiple sensor redundancy rather than absolute sensor accuracy. Multispectral sensors have the potential to be deployed relatively inexpensively if these technical issues can be resolved.

In our pilot study the digital camera images were downloaded manually, but as described by Gobbett et al. (2013) in an operational system the cameras could be solar powered and deliver data across a network that had sufficient bandwidth, particularly if daily image capture rather than every 30 minutes was found to be adequate. Testing the technology around sending image data across the network in this way was not the focus of this pilot deployment, but we illustrate the utility of such an approach by our transmission of the multispectral and soil moisture sensor data via a WSN.

We showed that a single image selected in the middle of the day was sufficient for seasonal monitoring, but that camera images from other times of the day were also useful for investigating unexpected data from the other sensors. The selection of camera images from the middle of the day was made to minimize illumination changes between images, and used an automated white balance setting on the camera following that used in (e.g. Macfarlane and Ogden, 2012). Other studies have used a manual/fixed white balance in order to minimize changes in illumination (Toomey et al., 2015;Sonnentag et al., 2012) and its use is recommended by the Phenocam network (http://phenocam.sr.unh.edu/webcam/). This aspect could be investigated further in future deployments, as it may enable even stronger correlations to be derived from the digital imagery.

There were benefits to having both multispectral sensors and digital cameras as they complement each other in data interpretation. In an operational setting with cost constraints, a single digital camera could be used to give visual feedback on pasture status to the producer, while using a wide deployment of spectral sensors as the main data source. In our study, the separate soil moisture sensors at each node were used to aid in data interpretation. Additional precipitation information could also be provided by the addition of a low cost rainfall sensor to alleviate the necessity of using rainfall data from non-local meteorological stations.

4.7. Overcoming the limitations of proximal sensors in heterogeneous pastures

We have been explicit in this study that we did not expect to capture the heterogeneity of tropical pastures with just the 2 sensors used in the pilot deployment, as assessing the spatial heterogeneity of the pastures was not the project's goal. The two nodes were intentionally placed in an area of the paddock that was as similar as possible at deployment, and the fencing of one node was aimed only at providing a range of pasture heights. An important question about the use of proximal sensors mounted on static nodes is whether the spatial heterogeneity of the pastures is adequately captured by the small area on the ground that the sensors observe, assuming an appropriate number of sensors are deployed. The small FOV of an individual sensor is in contrast to the spatially-extensive data obtained from satellite and airborne sensing platforms, and more recently from mobile platforms such as ground vehicles (e.g. King et al., 2010) helicopters, unmanned aerial vehicles (UAV) (e.g. Von Bueren et al., 2015), and robotic setups to move sensors (Hamilton et al., 2007). In an operational deployment of sensors it may not be necessary to spatially sample the landscape exhaustively, as occurs from an imaging platform such as a satellite; the landscape only needs to be sampled with the number of nodes and their spatial arrangement suitable to capture the spatial pattern in the particular landscape. This includes considerations such as whether the spatial pattern in the pastures is relatively stable, as is more common in temperate pastures, or is more clumped and heterogeneous as is common in tropical pastures. Spatially heterogeneous pastures can also result from pasture management such as re-seeding. The assessment of landscape spatial pattern at multiple scales is a broad topic; a good overview can be found in McCoy (2005), and a more detailed example in Chen et. al, (2012).

Options for addressing these spatial sampling concerns of point-based proximal sensors in an operational system include placing multiple sensors strategically in key paddock zones such that the sensors capture the range of paddock variability. Remote sensing images, even if captured only once or twice per year, could be used to aid in the delineation of suitable zones in conjunction with local farmer knowledge. Data from this setup could then be aggregated up to the scale of a farm management unit to create a robust time-series of observations. Alternatively, the sensors could be mounted on a mobile platform that monitors the pastures along a series of waypoints at set times of the day. Unlike the set revisit times of satellite-based remotely sensed images, helicopters and UAVs have the potential to capture data under a more flexible acquisition schedule. However, data from these non-satellite platforms have more complex processing requirements due to the stability of the imaging platform and the capture of strips of image data in separate flight lines. Increasingly, these processing limitations of mobile platforms are being mitigated by advances in automating image processing (Colomina and Molina, 2014), but they still have the limitation of providing intermittent rather than continuous monitoring. More importantly, while capturing raw data from these systems is relatively easy, creating an operational system to convert the data to something the producer can use for decisions making is complex.

While there are limitations of using point-based sensors for monitoring heterogeneous tropical pastures, this is balanced by the benefits of having a near real-time continuous data stream for monitoring. For example, an ideal pasture monitoring system would combine data from multiple sources; proximal sensing data for repeated and continuous monitoring of the pastures, and remote sensing images collected at a limited number of times when a spatial assessment of pastures is required. An automatic sensor system could also be set up to trigger a notification to a smart phone or tablet, when a critical threshold in feed availability or bare ground has been reached. These data sources could also be combined with other precision farm management technologies, such as walk over weighing (González et al., 2014), and emerging low power sensor network systems (e.g. http://www.taggle.com.au). For these combined sensor technologies to be used on-farm outside of the current research pilot deployment would require future technical development to streamline their installation and operational use.

5. Conclusions

This project has demonstrated the successful deployment of multiple proximal sensors to monitor tropical pastures in an operational beef production system over 18 months. In our pilot deployment we had a number of technical issues that limited the amount of sensor data that was of suitable quality for comparison to the field observations. Due to the uncertainty in the field observations, the relationships developed between sensor and field data are not confirmational and should be used only to inform the design of future work.

The design of a new sensor deployment would depend on the project goals. For example, to deliver operational data to farmers for decision making, to validate satellite images, to test the design of sampling schemes using many low-cost sensors, or to use proximal sensors for monitoring an area for degradation. As a result of this pilot project, we recommend a number of considerations for a full deployment of multiple proximal sensors for monitoring tropical pastures:

Sensor choice

- Utilising a multispectral sensor construction such as the Skye SKR 1860D sensor (Skye-Instruments, 2013) will mitigate many of the technical issues we had with the multispectral sensor. The gross failure of our multispectral sensor model due to moisture entry was exacerbated by the tropical conditions, but these issues are likely to be mitigated by newer model sensors. Using multispectral sensors with an improved design should also provide more robust data collection and require less stringent data filtering.
- Including a multispectral sensor band in the upper SWIR range would help capture the changing balance between PV and NPV across the season.
- We found the digital cameras to be more robust at acquiring data compared to the multispectral sensors. However, the multispectral sensors captured more characteristics of the pastures than just the green vegetation component. We therefore recommend having a system with both sensor types, with the additional benefit of assisting in data interpretation and troubleshooting technical issues.
- The soil moisture sensors provided valuable information about the soil moistures status. Having an on-site weather station would also benefit data analysis, particularly for rainfall which is highly localised. A single weather station or rain gauge should be sufficient if the area where the sensors are deployed is small enough to not have widely varying rainfall.

Sensor Deployment

- Issues such as insects and dust are common to sensor deployments in all environments, and while mitigated by sensor maintenance, would need to be addressed in an automated fashion if multiple autonomous sensors are to be deployed over long time periods.
- Regular maintenance, whether manual or automated, should include re-calibration of sensors due to degradation over time, and the cross-calibration needs of deployments of multiple sensors.
- Ideally there would be a number of sensors deployed which capture the pasture heterogeneity of a particular deployment.
- There are also many technical choices that could be explored in a larger project, such as transferring image data across the WSN, or processing data at the sensor node.

Data processing and filtering

- Data processing steps such as noise filtering and the necessity of calibration are common to all spectral sensor deployments, and should be considered part of the operational deployment methodology.
- Focussing data extraction on the middle part of the day is recommended to reduce differences in illumination. Reducing the period when the sensors are acquiring data will also minimise the volume of data to be collected, and the corresponding energy, data storage, and transfer requirements of the deployment.

Optimising resources

- For future sensor deployments in tropical pastures for on-farm decision making, we recommend limiting data acquisition to the critical periods of vegetation growth during the wet season and into the start of the dry season, which will also simplify the deployment resource requirements.

Field data collections

- We recommend the use a non-destructive sampling method such as BOTANAL, which includes a protocol for assessing and maintaining accuracy of visual measurements of pasture biomass and composition (Tothill et al., 1992;Orchard et al., 2000). Such a method would improve the accuracy and precision of the field data, although at a much higher resource requirement. This time requirement may be mitigated if the data collections are focussed at a shorter period during the year, rather than across the whole year such as in this current study.

Overall, we found that the limitations of proximal sensors mounted on static nodes are balanced by their ability to monitor continually and deliver near real-time data without being affected by clouds, and their potentially for being deployed autonomously in remote locations in an extensive grazing system. These results show that proximal sensors, particularly when multiple sensors are combined in the same deployment, have the ability to provide a valuable alternative to physical assessments of pasture. Continuous monitoring permits the rapid identification of changing conditions and informed and timely management decision-making on-farm. Our pilot project supports the design of future deployments in this environment and their potential for operational use.

Author contribution

The field experiments were designed by RNH (25%), DLG (25%), LAG (25%), and GBH (25%).

The field work was done by SLM (50%), LAG (20%), GBH (20%), RNH (5%), and DLG (5%).

The data cleaning and synthesis was done by RNH (40%), DLG (35%), and SLM (25%).

The design and implementation of the data analysis was done by RNH (50%) and DLG (50%).

The manuscript and figures were prepared by RNH (70%) and DLG (15%), with contributions from all co-authors, LAG (5%), GBH (5%), and SLM (5%).

Acknowledgements

We gratefully acknowledge the CSIRO Sustainable Agricultural Flagship who funded this research, and Noboru Ota, Chris Crossman, and Philip Valencia for technical support, as well as two anonymous reviewers for their extremely helpful suggestions.

With particular thanks to the statistical advice provided by Prof. Mark S. Handcock (Department of Statistics, University of California at Los Angeles). The first author is especially grateful for his assistance, as it proved that number 2 is a better predictor than number 6.

References

Allen, M. F., Vargas, R., Graham, E. A., Swenson, W., Hamilton, M., Taggart, M., Harmon, T. C., Rat'Ko, A., Rundel, P., Fulkerson, B., and Estrin, D.: Soil Sensor Technology: Life within a Pixel, BioScience, 57, 859-867, 10.1641/B571008, 2007.

Asner, G. P.: Biophysical and biochemical sources of variability in canopy reflectance, Remote Sensing of Environment, 64, 234-253, 1998.

Baldridge, A. M., Hook, S. J., Grove, C. I., and Rivera, G.: The ASTER spectral library version 2.0, Remote Sens. Environ., 113, 711-715, 10.1016/j.rse.2008.11.007, 2009.

Balzarolo, M., Anderson, K., Nichol, C., Rossini, M., Vescovo, L., Arriga, N., Wohlfahrt, G., Calvet, J.-C., Carrara, A., Cerasoli, S., Cogliati, S., Daumard, F., Eklundh, L., Elbers, J. A., Evrendilek, F., Handcock, R. N., Kaduk, J., Klumpp, K., Longdoz, B., Matteucci, G., Meroni, M., Montagnani, L., Ourcival, J.-M., Sánchez-Cañete, E. P., Pontailler, J.-Y., Juszczak, R., Scholes, B., and Martín, M. P.: Ground-based optical measurements at European flux sites: A review of methods, instruments and current controversies, Sensors, 11, 7954-7981, 2011.

Basu, S., and Meckesheimer, M.: Automatic outlier detection for time series: An application to sensor data, Knowledge and Information Systems, 11, 137-154, 2007.

Bennett, L. T., Judd, T. S., and Adams, M. A.: Close-range vertical photography for measuring cover changes in perennial grasslands, Journal of Range Management, 53, 634-641, 2000.

Booth, D. T., Cox, S. E., Fifield, C., Phillips, M., and Willlamson, N.: Image analysis compared with other methods for measuring ground cover, Arid Land Research and Management, 19, 91-100, 2005.

Carpenter, J.: Bootstrap Methods and their Application. Eds. A. C. Davison and D. V. Hinkley. Cambridge University Press. 1997. Pp. x+582. £24.95 (paperback), £70.00 (hardback). ISBN 0 521 57391 2 (hardback), 0 521 57471 4 (paperback), Epidemiology and Infection, 121, 485-485, 10.1017/S0950268898001241, 1998.

Catchpole, W. R., and Wheeler, C. J.: Estimating plant biomass: A review of techniques, Austral Ecology, 17, 121-131, 10.1111/j.1442-9993.1992.tb00790.x, 1992.

Chen, B., Coops, N. C., Fu, D., Margolis, H. A., Amiro, B. D., Black, T. A., Arain, M. A., Barr, A. G., Bourque, C. P. A., Flanagan, L. B., Lafleur, P. M., McCaughey, J. H., and Wofsy, S. C.: Characterizing spatial representativeness of flux tower eddy-covariance measurements across the Canadian Carbon Program Network using remote sensing and footprint analysis, Remote Sens. Environ., 124, 742-755, http://dx.doi.org/10.1016/j.rse.2012.06.007, 2012.

Collins, S. L., Bettencourt, L. M. A., Hagberg, A., Brown, R. F., Moore, D. I., Bonito, G., Delin, K. A., Jackson, S. P., Johnson, D. W., Burleigh, S. C., Woodrow, R. R., and McAuley, J. M.: New opportunities in ecological sensing using wireless sensor networks, Frontiers in Ecology and the Environment, 4, 402-407, 10.1890/1540-9295(2006)4[402:noiesu]2.0.co;2, 2006.

Colomina, I., and Molina, P.: Unmanned aerial systems for photogrammetry and remote sensing: A review, ISPRS Journal of Photogrammetry and Remote Sensing, 92, 79-97, http://dx.doi.org/10.1016/j.isprsjprs.2014.02.013, 2014.

Department of Resources Northern Territory Australia, and Meat and Livestock Australia: Cattle and land management best practices in the Top End region : 2011, Northern Territory Government. Dept. of Resources, 2012.

Eklundh, L., Jin, H., Schubert, P., Guzinski, R., Heliasz, M., Naturvetenskap, Institutionen för naturgeografi och, e., Science, Geocentrum, II, Lunds, u., Geocentre, II, Lund, U., Dept of Physical, G., Ecosystem, S., Biologisk-geovetenskapliga, v., Section of, B., and Earth, S.: An optical sensor network for vegetation phenology monitoring and satellite data calibration, Sensors (Basel, Switzerland), 11, 7678-7709, 10.3390/s110807678, 2011.

Ewing, R. P., and Horton, R.: Quantitative color image analysis of agronomic images, Agronomy Journal, 91, 148-153, 1999.

Flynn, E. S., Dougherty, C. T., and Wendroth, O.: Assessment of pasture biomass with the normalized difference vegetation index from active ground-based sensors, Agronomy Journal, 100, 114-121, 10.2134/agronj2006.0363, 2008.

Friedel, M. H., Chewings, V. H., and Bastin, G. N.: The Use of Comparative Yield and Dry-Weight-Rank Techniques for Monitoring Arid Rangeland, Journal of Range Management, 41, 430-435, 10.2307/3899584, 1988.

Gamon, J. A.: Reviews and Syntheses: Optical sampling of the flux tower footprint, Biogeosciences, 12, 4509-4523, 10.5194/bg-12-4509-2015, 2015.

Gitelson, A. A., Kaufman, Y. J., and Merzlyak, M. N.: Use of a green channel in remote sensing of global vegetation from EOS- MODIS, Remote Sens. Environ., 58, 289-298, 1996.

Gobbett, D., Handcock, R. N., Zerger, A., Crossman, C., Valencia, P., Wark, T., and Davies, M.: Prototyping an Operational System with Multiple Sensors for Pasture Monitoring, Journal of Sensor and Actuator Networks, 2, 388-408, 2013.

González, L. A., Bishop-Hurley, G., Henry, D., and Charmley, E.: Wireless sensor networks to study, monitor and manage cattle in grazing systems, Anim. Prod. Sci., 54, 1687-1693, http://dx.doi.org/10.1071/AN14368, 2014.

Guerschman, J. P., Hill, M. J., Renzullo, L. J., Barrett, D. J., Marks, A. S., and Botha, E. J.: Estimating fractional cover of photosynthetic vegetation, non-photosynthetic vegetation and bare soil in the Australian tropical savanna region upscaling the EO-1 Hyperion and MODIS sensors, Remote Sensing of Environment, 113, 928-945, 2009.

Hamilton, M. P., Graham, E. A., Rundel, P. W., Allen, M. F., Kaiser, W., Hansen, M. H., and Estrin, D. L.: New Approaches in Embedded Networked Sensing for Terrestrial Ecological Observatories, Environmental Engineering Science, 24, 192-204, 10.1089/ees.2006.0045, 2007.

Handcock, R. N., Mata, G., and Gherardi, S. G.: Combining spectral information aggregated to the paddock scale with knowledge of on-farm practices will enhance remote sensing methods for intensively managed dairy pastures, 14th Australian Remote Sensing and Photogrammetry Conference, Darwin, Australia, 29 Sept. - 3rd. Oct. 2008, 2008.

Harrell, F. E., Lee, K. L., and Mark, D. B.: MULTIVARIABLE PROGNOSTIC MODELS: ISSUES IN DEVELOPING MODELS, EVALUATING ASSUMPTIONS AND ADEQUACY, AND MEASURING AND REDUCING ERRORS, Statistics in Medicine, 15, 361-387, 10.1002/(SICI)1097-0258(19960229)15:4<361::AID-SIM168>3.0.CO;2-4, 1996.

Harris, A., Gamon, J. A., Pastorello, G. Z., and Wong, C. Y. S.: Retrieval of the photochemical reflectance index for assessing xanthophyll cycle activity: a comparison of near-surface optical sensors, Biogeosciences, 11, 6277-6292, 10.5194/bg-11-6277-2014, 2014.

Hastie, T. J., and Tibshirani, R.: Generalized additive models, Book, Whole, Chapman and Hall, New York;London;, 1990.

Holben, B. N.: Characteristics of maximum-value composite images from temporal AVHRR data, International Journal of Remote Sensing, 7, 1417-1434, 10.1080/01431168608948945, 1986.

Huemmrich, K. F., Black, T. A., Jarvis, P. G., McCaughey, J. H., and Hall, F. G.: High temporal resolution NDVI phenology from micrometeorological radiation sensors, Journal of Geophysical Research: Atmospheres, 104, 27935-27944, 1999.

Jackson, R. D., and Huete, A. R.: Interpreting vegetation indices, Preventive Veterinary Medicine, 11, 185-200, http://dx.doi.org/10.1016/S0167-5877(05)80004-2, 1991.

Jeffery, S. R., Alonso, G., Franklin, M. J., Wei, H., and Widom, J. A.: Pipelined Framework for Online Cleaning of Sensor Data Streams, 22nd International Conference on Data Engineering, ICDE'06, Atlanta, GA, USA, 3–7 April 2006, 2006.

Johnson, D., Vulfson, M., Louhaichi, M., and Harris, N.: Vegmeasure v1.6 user's manual, Department of Rangeland Resources, Oregon State University, Corvallis, Oregon, USA, 2003.

Karcher, D. E., and Richardson, M. D.: Batch analysis of digital images to evaluate turfgrass characteristics, Crop Science, 45, 1536-1539, 2005.

King, W., Rennie, G. M., Dalley, D. E., Dynes, R. A., and Upsdell, M. P.: Pasture mass estimation by the C-DAX pasture meter: regional calibrations for New Zealand, Proceedings of the Australasian Dairy Science Symposium, Caxton Press, 233-238 pp., 2010.

Liu, H., Shah, S., and Jiang, W.: On-line outlier detection and data cleaning, Computers and Chemical Engineering, 28, 1635-1647, 2004.

Lo, F., Wheeler, M. C., Meinke, H., and Donald, A.: Probabilistic forecasts of the onset of the north Australian wet season, Mon. Weather Rev., 135, 3506-3520, 10.1175/mwr3473.1, 2007.

Louhaichi, M., Borman, M. M., and Johnson, D. E.: Spatially located platform and aerial photography for documentation of grazing impacts on wheat, Geocarto International, 16, 65-70, 2001.

Lukina, E. V., Stone, M. L., and Raun, W. R.: Estimating vegetation coverage in wheat using digital images, Journal of Plant Nutrition, 22, 341-350, 1999.

Macfarlane, C., and Ogden, G. N.: Automated estimation of foliage cover in forest understorey from digital nadir images, Methods in Ecology and Evolution, 3, 405-415, 10.1111/j.2041-210X.2011.00151.x, 2012.

McCoy, R. M.: Field methods in remote sensing, Book, Whole, Guilford Press, New York, 2005.

Myneni, R. B., and Williams, D. L.: On the relationship between FAPAR and NDVI, Remote Sens. Environ., 49, 200-211, http://dx.doi.org/10.1016/0034-4257(94)90016-7, 1994.

Ni, K., Ramanathan, N., Chehade, M. N. H., Balzano, L., Nair, S., Zahedi, S., Kohler, E., Pottie, G., Hansen, M., and Srivastava, M.: Sensor network data fault types, ACM Transactions on Sensor Networks, 5, 1-29, 2009.

O'Reagain, P., Scanlan, J., Hunt, L., Cowley, R., and Walsh, D.: Sustainable grazing management for temporal and spatial variability in north Australian rangelands - A synthesis of the latest evidence and recommendations, Rangeland J., 36, 223-232, 10.1071/RJ13110, 2014.

Orchard, B. A., Cullis, B. R., Coombes, N. E., Virgona, J. M., and Klein, T.: Grazing management studies within the Temperate Pasture Sustainability Key Program: Experimental design and statistical analysis, Australian Journal of Experimental Agriculture, 40, 143-154, 10.1071/EA98005, 2000.

Payero, J. O., Neale, C. M. U., and Wright, J. L.: Comparison of eleven vegetation indices for estimating plant height of alfalfa and grass, Applied Engineering in Agriculture, 20, 385-393, 2004.

Pearson, R. L., Tucker, C. J., and Miller, L. D.: Spectral mapping of shortgrass prarie biomass, Photogramm. Eng. Remote Sens., 42, 317-323, 1976.

Peddle, D. R., Peter White, H., Soffer, R. J., Miller, J. R., and LeDrew, E. F.: Reflectance processing of remote sensing spectroradiometer data, Computers and Geosciences, 27, 203-213, 10.1016/S0098-3004(00)00096-0, 2001.

Peters, S. C., and Freedman, D. A.: Some Notes on the Bootstrap in Regression Problems, Journal of Business & Economic Statistics, 2, 406-409, 1984.

Pullanagari, R. R., Yule, I. J., Tuohy, M. P., Hedley, M. J., Dynes, R. A., and King, W. M.: In-field hyperspectral proximal sensing for estimating quality parameters of mixed pasture, Precision Agric, 13, 351-369, 10.1007/s11119-011-9251-4, 2012.

Queensland Department of Primary Industries: Pasture Photo Standards CD-ROM, 2003.

Richardson, A. D., Jenkins, J. P., Braswell, B. H., Hollinger, D. Y., Ollinger, S. V., and Smith, M. L.: Use of digital webcam images to track spring green-up in a deciduous broadleaf forest, Oecologia, 152, 323-334, 2007.

Richter, K., Atzberger, C., Hank, T. B., and Mauser, W.: Derivation of biophysical variables from Earth observation data: validation and statistical measures, JOURNAL OF APPLIED REMOTE SENSING, 6, 10.1117/1.JRS.6.063557, 2012.

Sakowska, K., Vescovo, L., Marcolla, B., Juszczak, R., Olejnik, J., and Gianelle, D.: Monitoring of carbon dioxide fluxes in a subalpine grassland ecosystem of the Italian Alps using a multispectral sensor, Biogeosciences, 11, 4695-4712, 10.5194/bg-11-4695-2014, 2014.

Sanderson, M. A., Rotz, C. A., Fultz, S. W., and Rayburn, E. B.: Estimating Forage Mass with a Commercial Capacitance Meter, Rising Plate Meter, and Pasture Ruler, Agronomy Journal, 93, 1281, 10.2134/agronj2001.1281, 2001.

Serrano, J. M., Shahidian, S., and Marques da Silva, J. R.: Monitoring pasture variability: optical OptRx® crop sensor versus Grassmaster II capacitance probe, Environmental Monitoring and Assessment, 188, 1-17, 10.1007/s10661-016-5126-5, 2016.

Skye-Instruments: Application Notes Sensors for NDVI Calculations, 21, Ddole Enterprise Park, Llandrindod Wells, Powys LD1 6DF, UK, 1, 2012a.

Skye-Instruments: SKR 1850D & 1850ND, SKR 1850D/A & 1850ND/A 4 Channel Sensor, 21, Ddole Enterprise Park, Llandrindod Wells, Powys LD1 6DF, UK, 1, 2012b.

Skye-Instruments: 4 Channel Sensor SKR 1860D & SKR 1860ND, 21, Ddole Enterprise Park, Llandrindod Wells, Powys LD1 6DF, UK, 1, 2013.

Sonnentag, O., Hufkens, K., Teshera-Sterne, C., Young, A. M., Friedl, M., Braswell, B. H., Milliman, T., O'Keefe, J., and Richardson, A. D.: Digital repeat photography for phenological research in forest ecosystems, Agricultural and Forest Meteorology, 152, 159-177, 10.1016/j.agrformet.2011.09.009, 2012.

Steyerberg, E. W., Harrell Jr, F. E., Borsboom, G. J. J. M., Eijkemans, M. J. C., Vergouwe, Y., and Habbema, J. D. F.: Internal validation of predictive models: Efficiency of some procedures for logistic regression analysis, Journal of Clinical Epidemiology, 54, 774-781, 10.1016/S0895-4356(01)00341-9, 2001.

t'Mannetje, L., and Haydock, K. P.: The dry-weight-rank method of botanical analysis of pasture, Grass and Forage Science, 18, 268-275, 10.1111/j.1365-2494.1963.tb00362.x, 1963.

Toomey, M., Friedl, M. A., Frolking, S., Hufkens, K., Klosterman, S., Sonnentag, O., Baldocchi, D. D., Bernacchi, C. J., Biraud, S. C., Bohrer, G., Brzostek, E., Burns, S. P., Coursolle, C., Hollinger, D. Y., Margolis, H. A., McCaughey, H., Monson, R. K., Munger, J. W., Pallardy, S., Phillips, R. P., Torn, M. S., Wharton, S., Zeri, M., and Richardson, A. D.: Greenness indices from digital cameras predict the timing and seasonal dynamics of canopy-scale photosynthesis, Ecological Applications, 25, 99-115, 10.1890/14-0005.1, 2015.

Tothill, J., and Partridge, I. (Eds.) Monitoring grazing lands in northern AustraliaOccasional Publication No. 9, 98, 1998.

Tothill, J. C., Hargreaves, J. N. G., Jones, R. M., and McDonald, C. K.: BOTANAL – A Comprehensive Sampling and Computing Procedure for Estimating Pasture Yield and Composition. 1. Field Sampling, CSIRO Division of Tropical Crops & PasturesTropical Agronomy Technical Memorandum Number 78, 1992.

Trotter, M. G., Lamb, D. W., Donald, G. E., and Schneider, D. A.: Evaluating an active optical sensor for quantifying and mapping green herbage mass and growth in a perennial grass pasture, Crop & Pasture Science, 61, 389-398, 10.1071/CP10019, 2010.

Tucker, C. J.: Red and photographic infrared linear combinations for monitoring vegetation, Remote Sens. Environ., 8, 127-150, 10.1016/0034-4257(79)90013-0, 1979.

Tucker, C. J.: Remote sensing of leaf water content in the near infrared, Remote Sens. Environ., 10, 23-32, 1980.

Turner, D. P., Cohen, W. B., Kennedy, R. E., Fassnacht, K. S., and Briggs, J. M.: Relationships between leaf area index and Landsat TM spectral vegetation indices across three temperate zone sites, Remote Sens. Environ., 70, 52-68, 1999.

Von Bueren, S. K., Burkart, A., Hueni, A., Rascher, U., Tuohy, M. P., and Yule, I. J.: Deploying four optical UAV-based sensors over grassland: Challenges and limitations, Biogeosciences, 12, 163-175, 10.5194/bg-12-163-2015, 2015.

Weber, C., Schinca, D. C., Tocho, J. O., and Videla, F.: Passive field reflectance measurements, Journal of Optics A: Pure and Applied Optics, 10, 104020, 2008.

Wood, S. N.: Fast stable restricted maximum likelihood and marginal likelihood estimation of semiparametric generalized linear models, Journal of the Royal Statistical Society. Series B (Statistical Methodology), 73, 3-36, 10.1111/j.1467-9868.2010.00749.x, 2011.

Zerger, A., Viscarra Rossel, R. A., Swain, D. L., Wark, T., Handcock, R. N., Doerr, V. A. J., Bishop-Hurley, G. J., Doerr, E. D., Gibbons, P. G., and Lobsey, C.: Environmental sensor networks for vegetation, animal and soil sciences, International Journal of Applied Earth Observation and Geoinformation, 12, 303-316, 10.1016/j.jag.2010.05.001, 2010.

Zerger, A., Gobbett, D., Crossman, C., Valencia, P., Wark, T., Davies, M., Handcock, R. N., and Stol, J.: Temporal monitoring of groundcover change using digital cameras, International Journal of Applied Earth Observation and Geoinformation, 19, 266-275, 2012.

Zhang, Y., Meratnia, N., and Havinga, P. J. M.: Ensuring high sensor data quality through use of online outlier detection techniques, International Journal of Sensor Networks, 7, 141-151, 2010.

Zhao, D., Starks, P. J., Brown, M. A., Phillips, W. A., and Coleman, S. W.: Assessment of forage biomass and quality parameters of bermudagrass using proximal sensing of pasture canopy reflectance, Grassland Science, 53, 39-49, 10.1111/j.1744-697X.2007.00072.x, 2007.

Table 1 Vegetation indices calculated from the multispectral sensor data. ρ = reflectance (0 to 1).

Index Name	**Equation**	**Reference**	**Application for this study**
NDVI	$(\rho_{NIR} - \rho_{red}) / (\rho_{NIR} + \rho_{red})$	Tucker, 1979	Vegetation "vigour"
RatioNS34	$\rho_{NIR} / \rho_{lowerSWIR}$	e.g. Handcock et al., 2008	Proportion of PV and NPV/soil
NVI-GR	$(\rho_{green} - \rho_{red}) / (\rho_{green} + \rho_{red})$	Jackson and Huete, 1991	Vegetation "greenness"
gNDVI	$(\rho_{NIR} - \rho_{green}) / (\rho_{NIR} + \rho_{green})$	Gitelson et al., 1996	Vegetation "vigour" and "greenness"
NVI-SR	$(\rho_{lowerSWIR} - \rho_{red}) / (\rho_{lowerSWIR} + \rho_{red})$	Jackson and Huete, 1991	NPV/soil

Table 2 Criteria for filtering multispectral data for a day. Daily data were removed if they met any one of the following criteria.

Filtering Category	Data source	Criteria for deleting that day's data.
a) Spike in readings, or readings out of range, such as from a sensor issue	Night-time (00:00 to 01:00) median value of raw current.	One or more of the multispectral sensor bands in the paired node has a night-time median value of raw current > 10000 mV
		One or more of the multispectral sensor bands in the paired node has (raw current) > 3 STD from the band mean value.
	Day-time (12:00 to 13:00) median value of indices.	Data out of range (i.e. NDVI between 0 and 0.1) (Holben, 1986;Jackson and Huete, 1991).
		RatioNS34 drops to zero but within one day returns to the previous value.
b) Physical / logistical	Project metadata.	Work being done in the area under the node, sensors have been removed for maintenance or because the paddocks are being burned etc.
	Day-time (12:00 to 13:00) median value of raw current.	There are no data during the midday period from one or more of the sensors, which would restrict the calculation of a full suite of indices.
c) Appropriate data for the environment	Day-time (12:00 to 13:00) median value of indices.	NDVI < 0 (not likely in tropical pastures).
		RatioNS34 > 2, indicating a technical error as pastures should not have values in this range.
	.	(gNDVI < 0 or NVI-GR > - 0.10) and the date and weather data indicates that is in the dry season (i.e. the changing values are unlikely to be due to surface water.
d) Masking valid spectral data	Digital camera images, project metadata, and soil moisture data.	Surface water was identified by a combination of data sources and masked as it confounded the pasture signal.

Table 3 Of the 33 days of field data collections, the number of days, a) of field sampled data matching the filtered sensor data at each node, and b) matching filtered data combined for both nodes from each of the wet and dry seasons.

		Digital Cameras	Multispectral sensors
a)	Unfenced node	31	24
	Fenced node	32	18
b)	Wet Season	25	12
	Dry Season	38	30
	All year	63	42

Table 4 Bias-adjusted bootstrap point estimates of R^2 and (in parenthesis, the lower and upper bound of the corresponding 95% pivotal bootstrap confidence intervals), for all GAM combinations of sensor-derived indices and a) TotalBiomass, b) %BareGround, c) %Litter2D, d) %TotalVegetation2D, e) %Green3D, f) %Green2D, and g) VegetationHeight. See Figure 8 for graphs comparing these results.

Dependent variable	**Independent variable**	**All data**	**Wet season**	**Dry season**
a) TotalBiomass	GLA	0.07 (0.00, 0.19)	0.21 (0.00, 0.51)	-0.02 (0.00, 0.14)
	RatioNS34	0.15 (0.00, 0.38)	0.18 (0.00, 0.65)	0.02 (0.00, 0.28)
	NVI-SR	0.08 (0.00, 0.30)	0.72 (0.28, 0.98)	0.07 (0.00, 0.28)
	NVI-GR	0.21 (0.00, 0.43)	0.14 (0.00, 0.63)	0.17 (0.00, 0.40)
	NDVI	0.16 (0.00, 0.36)	0.49 (0.00, 0.87)	-0.03 (0.00, 0.13)
	gNDVI	-0.04 (0.00, 0.10)	0.58 (0.00, 0.93)	-0.11 (-0.03, 0.0)
b) %BareGround	GLA	0.03 (0.00, 0.10)	0.26 (0.00, 0.58)	0.05 (0.00, 0.13)
	RatioNS34	0.11 (0.00, 0.25)	0.20 (0.00, 0.65)	0.04 (0.00, 0.22)
	NVI-SR	0.10 (0.00, 0.28)	0.53 (0.00, 0.88)	0.17 (0.00, 0.34)
	NVI-GR	0.13 (0.00, 0.33)	-0.05 (0.00, 0.53)	0.26 (0.00, 0.45)
	NDVI	0.18 (0.00, 0.37)	0.45 (0.00, 0.79)	0.13 (0.00, 0.31)
	gNDVI	0.01 (0.00, 0.13)	0.65 (0.09, 0.92)	-0.06 (0.00, 0.03)
c) %Litter2D	GLA	0.24 (0.06, 0.39)	0.31 (0.00, 0.57)	0.11 (0.00, 0.30)
	RatioNS34	-0.01 (0.00, 0.13)	0.06 (0.00, 0.54)	-0.08 (-0.03, 0.00)
	NVI-SR	0.07 (0.00, 0.25)	-0.10 (0.00, 0.55)	-0.09 (0.00, 0.04)
	NVI-GR	0.19 (0.00, 0.42)	0.09 (0.00, 0.64)	0.10 (0.00, 0.31)
	NDVI	0.18 (0.00, 0.42)	0.05 (0.00, 0.64)	-0.01 (0.00, 0.21)
	gNDVI	0.13 (0.00, 0.36)	-0.25 (0.00, 0.57)	-0.06 (0.00, 0.09)
d) %TotalVegetation2D	GLA	0.17 (0.00, 0.31)	0.52 (0.17, 0.75)	0.07 (0.00, 0.20)
	RatioNS34	0.04 (0.00, 0.19)	0.27 (0.00, 0.69)	-0.11 (-0.02, 0.00)
	NVI-SR	0.12 (0.00, 0.31)	0.56 (0.00, 0.92)	0.02 (0.00, 0.20)
	NVI-GR	0.22 (0.00, 0.46)	0.12 (0.00, 0.63)	0.19 (0.00, 0.41)
	NDVI	0.22 (0.00, 0.44)	0.49 (0.00, 0.87)	0.06 (0.00, 0.24)
	gNDVI	0.06 (0.00, 0.25)	0.47 (0.00, 0.89)	-0.03 (0.00, 0.08)
e) %Green3D	GLA	0.87 (0.80, 0.93)	0.77 (0.64, 0.87)	0.77 (0.57, 0.91)
	RatioNS34	0.10 (0.00, 0.35)	0.81 (0.53, 1.00)	0.01 (0.00, 0.26)
	NVI-SR	0.77 (0.60, 0.88)	0.59 (0.13, 0.87)	0.66 (0.37, 0.83)
	NVI-GR	0.66 (0.40, 0.84)	0.44 (0.00, 0.80)	0.51 (0.06, 0.80)
	NDVI	0.66 (0.41, 0.84)	0.59 (0.15, 0.86)	0.40 (0.00, 0.72)
	gNDVI	0.66 (0.43, 0.82)	0.68 (0.27, 0.89)	0.41 (0.01, 0.67)
f) %Green2D	GLA	0.86 (0.79, 0.92)	(na)	0.76 (0.52, 0.92)
	RatioNS34	0.05 (0.00, 0.30)	(na)	-0.07 (0.00, 0.16)
	NVI-SR	0.72 (0.55, 0.84)	(na)	0.58 (0.23, 0.77)
	NVI-GR	0.65 (0.36, 0.84)	(na)	0.44 (0.00, 0.75)
	NDVI	0.64 (0.39, 0.83)	(na)	0.42 (0.00, 0.74)
	gNDVI	0.63 (0.35, 0.79)	(na)	0.39 (0.00, 0.69)
g) VegetationHeight	GLA	0.24 (0.01, 0.41)	0.41 (0.00, 0.71)	0.09 (0.00, 0.23)
	RatioNS34	0.15 (0.00, 0.34)	0.31 (0.00, 0.77)	0.10 (0.00, 0.32)
	NVI-SR	0.33 (0.07, 0.52)	0.66 (0.19, 0.95)	0.28 (0.00, 0.50)
	NVI-GR	0.27 (0.00, 0.49)	0.49 (0.00, 0.90)	0.22 (0.00, 0.44)
	NDVI	0.25 (0.00, 0.45)	0.61 (0.12, 0.95)	0.06 (0.00, 0.27)
	gNDVI	0.06 (0.00, 0.23)	0.42 (0.00, 0.83)	-0.05 (0.00, 0.05)

Figure 1The unfenced node with (a) the paired multispectral sensors with the cosine diffusion filter fitted only to the upward-pointing sensor, **(**b) the digital camera, (c) solar panel power supply, and (d) relay hardware to send data to the WSN.

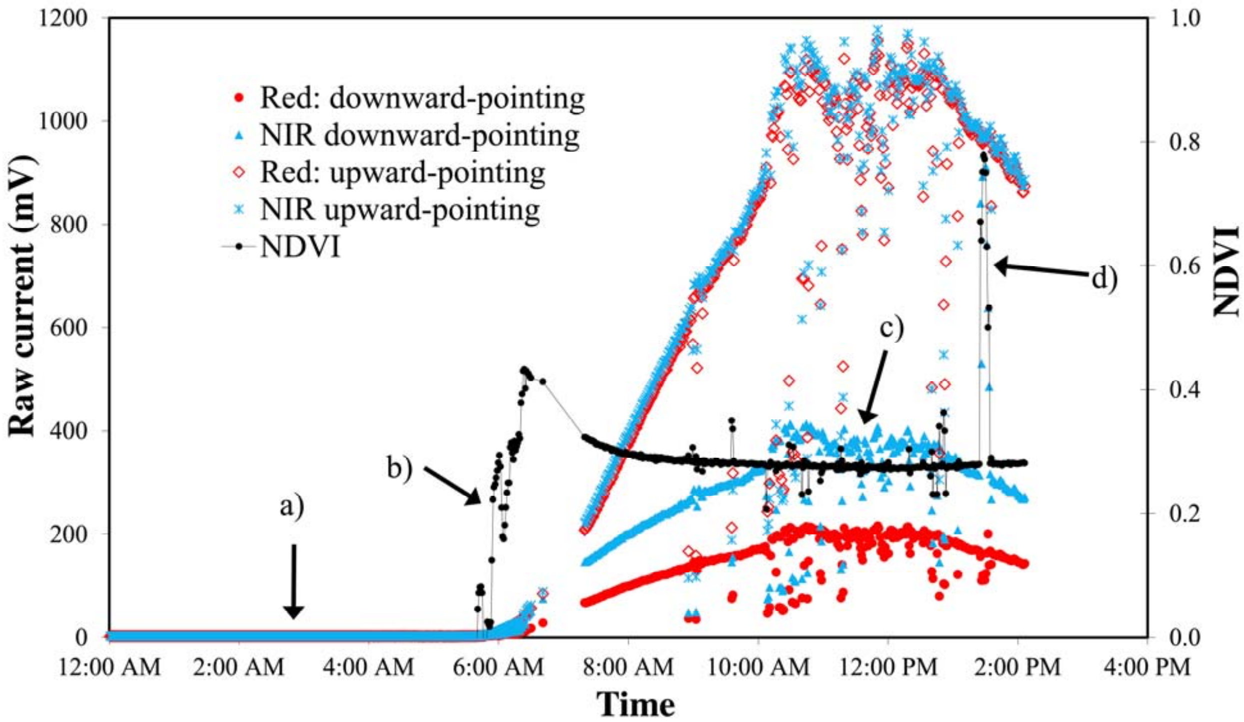

Figure 2 Example of the diurnal cycle of sensor data during the dry season when a large green leaf was held up to the multispectral sensors on the fenced node to test its response (4th October 2011). Note: for the NDVI a) night-time values, b) the ramp-up after dawn (approx. 6:30 AM), c) the relatively stable value for the middle part of the day, d) the spike in NDVI when the sensors recorded an elevation of NIR reflectance in response to green vegetation being held up to the sensor.

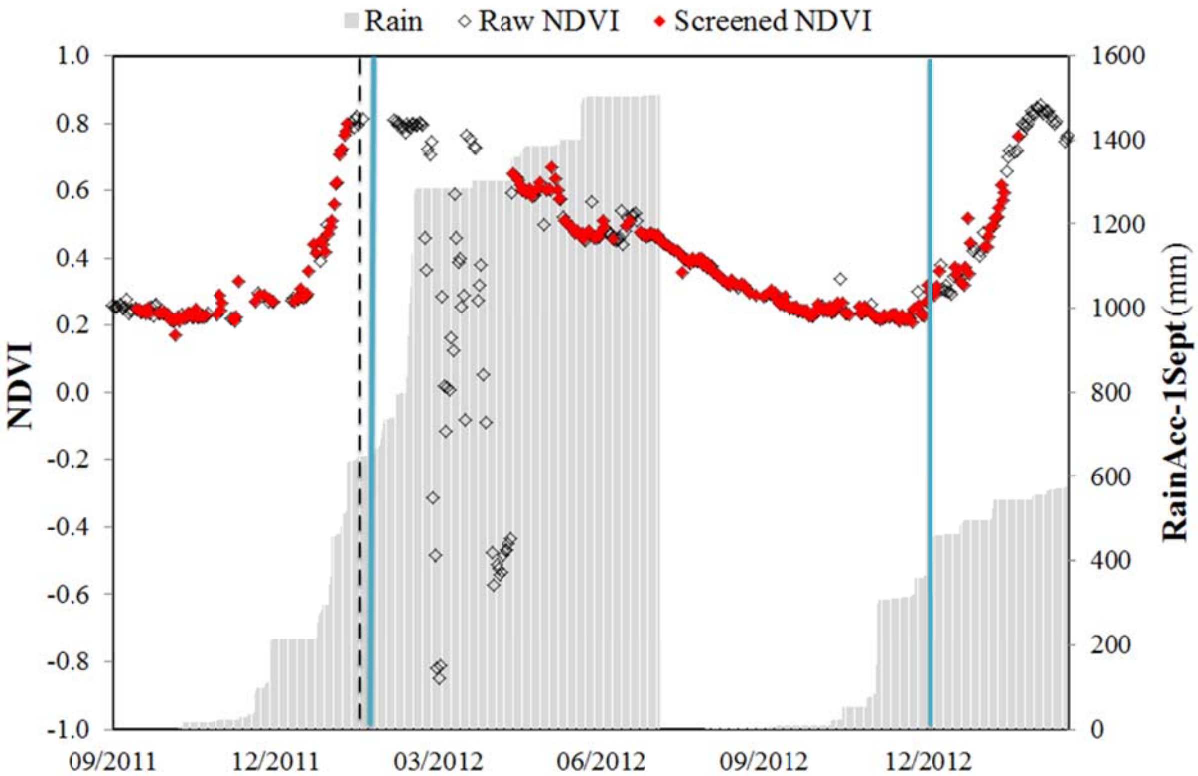

Figure 3 Time-series of NDVI values from the unfenced node showing the raw and screened NDVI and the accumulated precipitation since 1st September (mm) from "Townsville Airport" BoM weather station. The black dashed vertical line indicates the timing of the controlled burn, and the blue lines the start of the wet seasons.

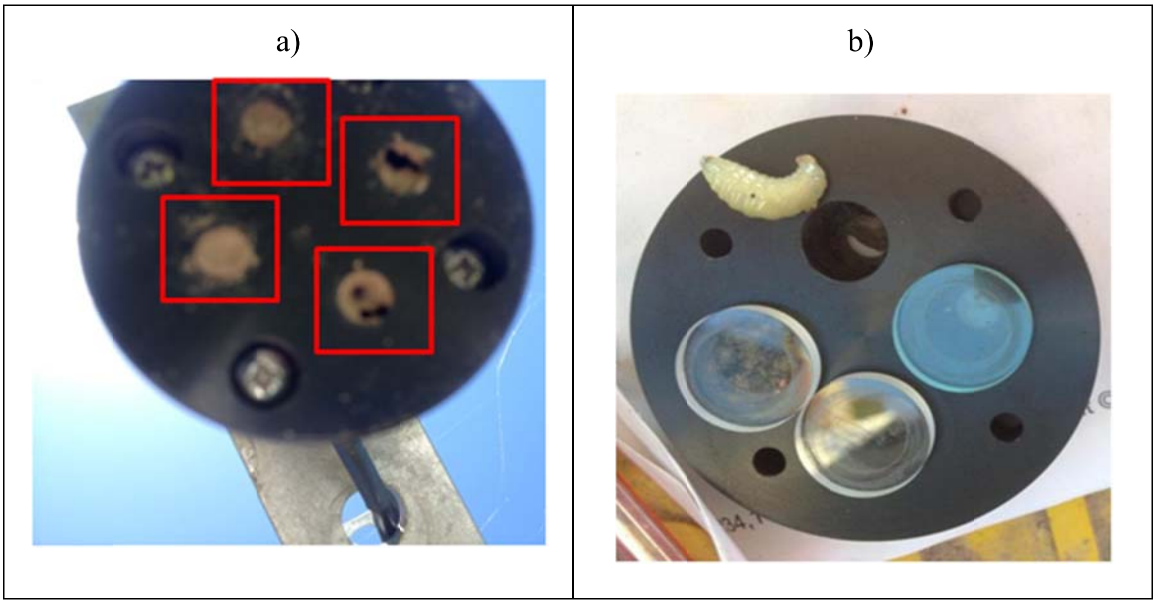

Figure 4 Skye multispectral sensors showing (a) mud wasps, and (b) wasp larvae in sensor tubes.

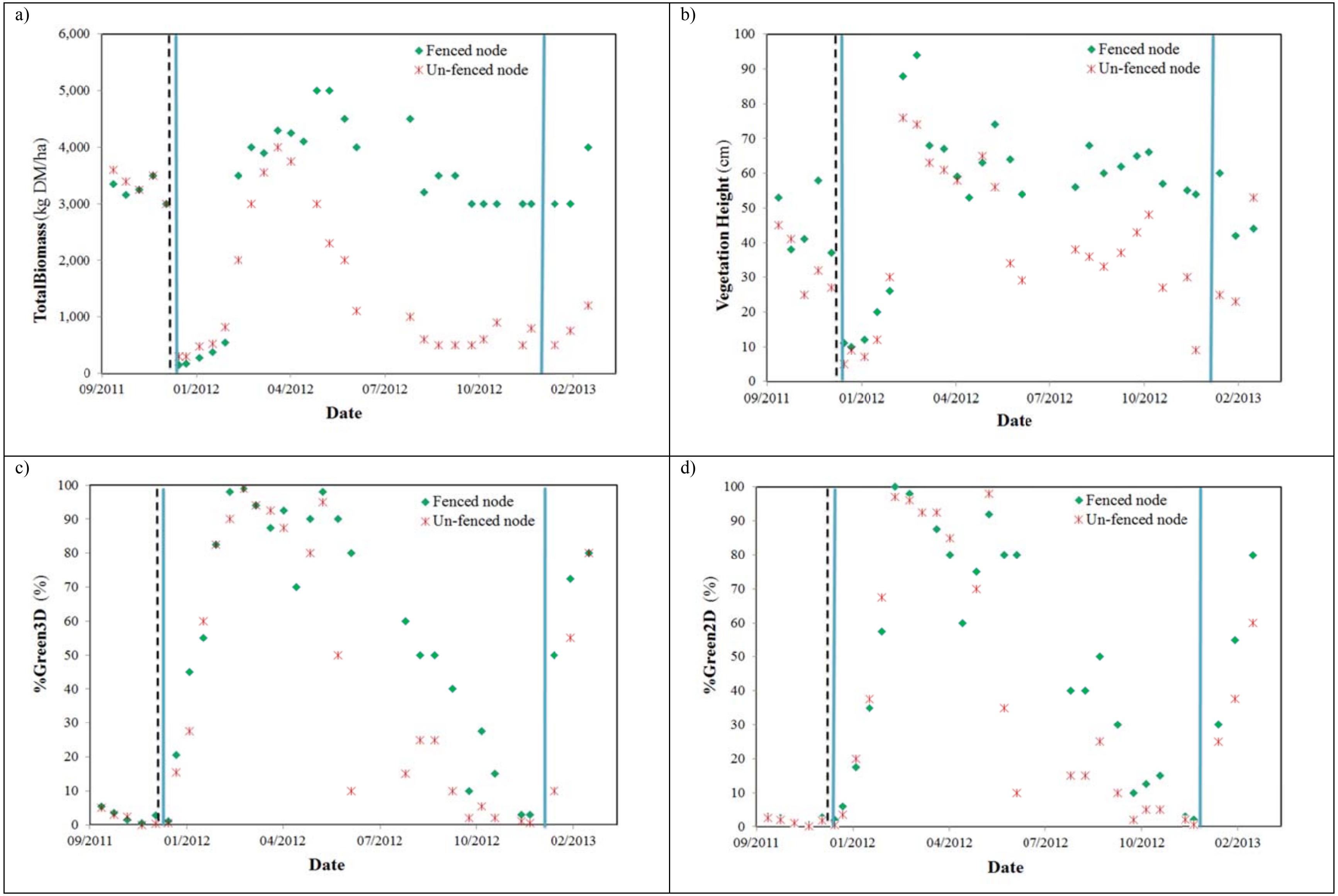
a)
Fenced node
Un-fenced node
TotalBiomass (kg DM/ha)
Date
b)
Fenced node
Un-fenced node
Vegetation Height (cm)
Date
c)
Fenced node
Un-fenced node
%Green3D (%)
Date
d)
Fenced node
Un-fenced node
%Green2D (%)
Date

Figure 5 Field observation time-series from the two nodes of (a) TotalBiomass, (b) VegetationHeight, (c) %Green3D, and (d) %Green2D. The black dashed line indicates the timing of the controlled burn, and the blue lines the start of the wet seasons.

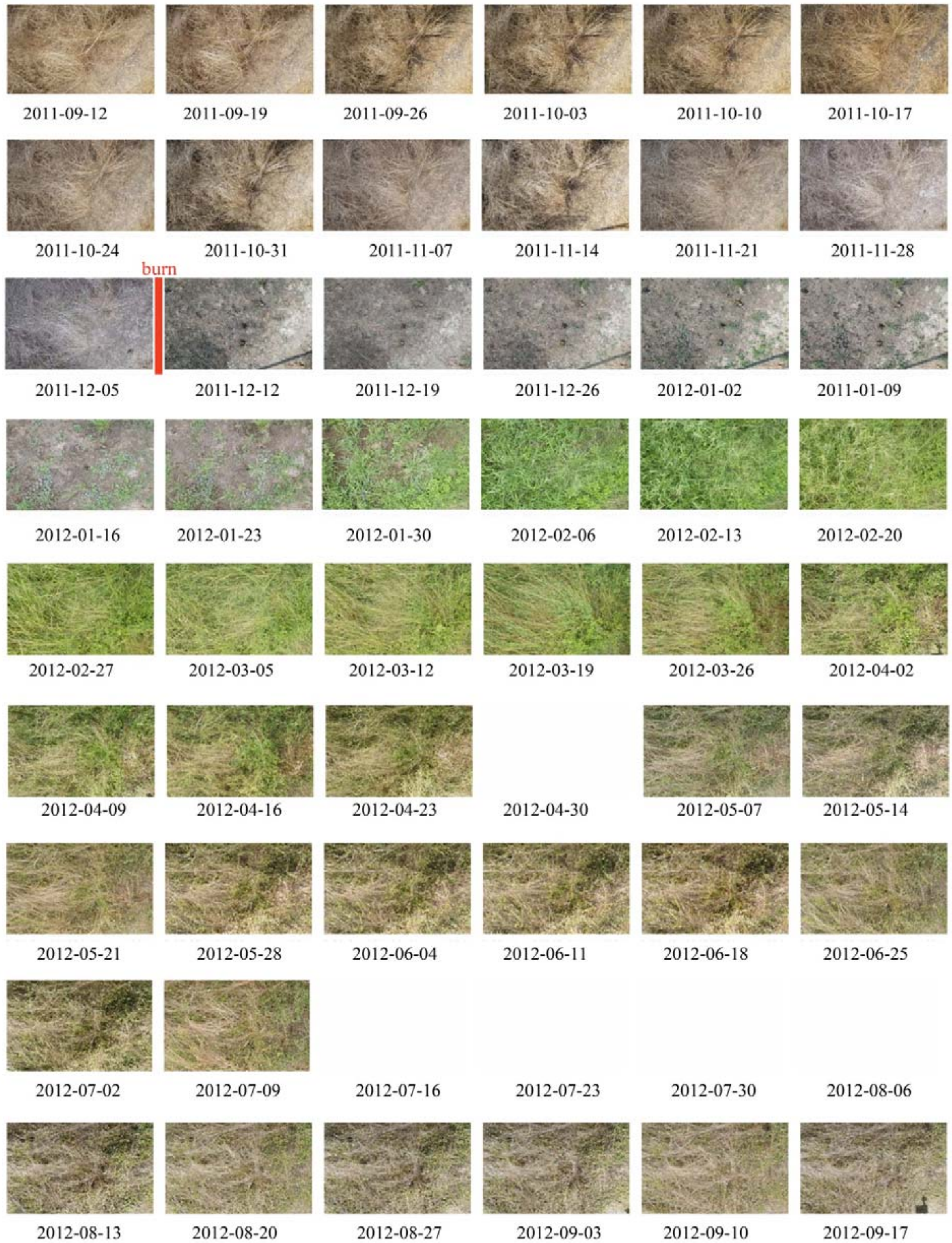

Figure 6 Time-series of a year of images from the digital camera at the fenced node, with each week represented by one image from approximately noon. The red line indicates the controlled burn in December 2011. Missing July images are due to a post-capture storage malfunction unrelated to the image capture.

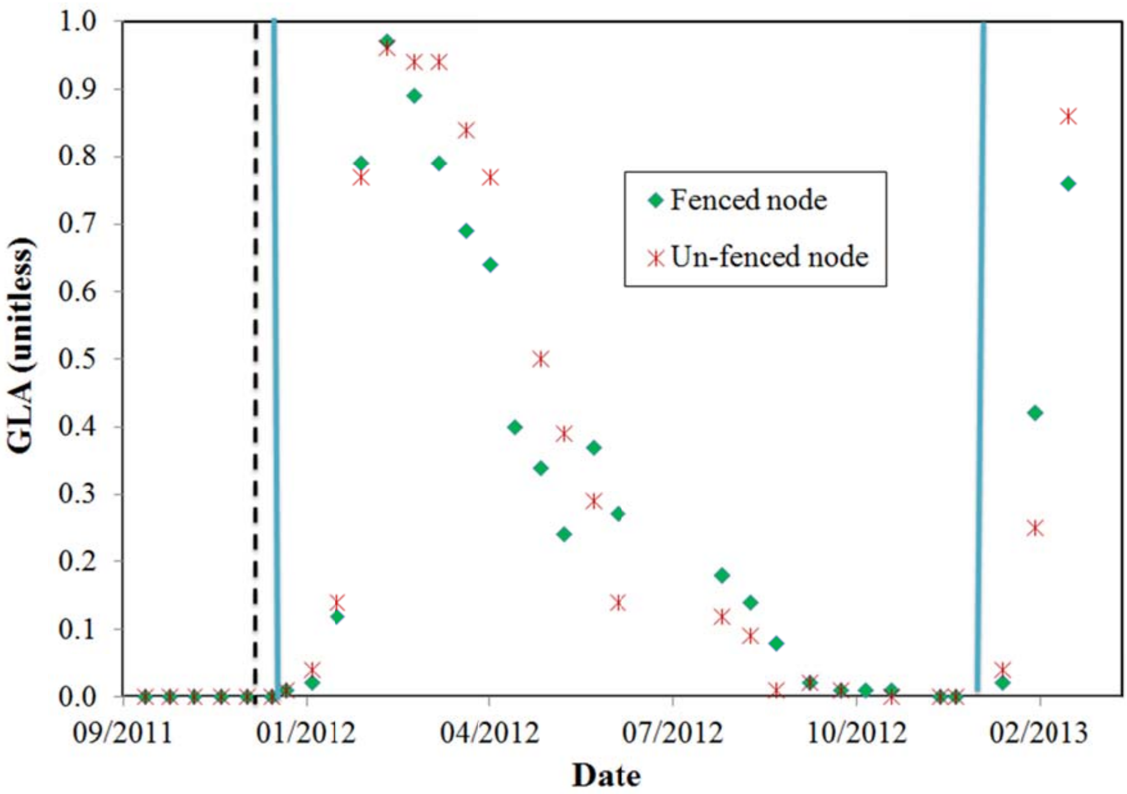

Figure 7 Time-series of the Green Leaf Algorithm (GLA) calculated from digital camera images at each node, using a daily image from approximately 12:00. The black dashed vertical line indicates the timing of the controlled burn, and the blue lines the start of the wet seasons. See Figure 5 for a time-series of the %Green3D and %Green2D field data.

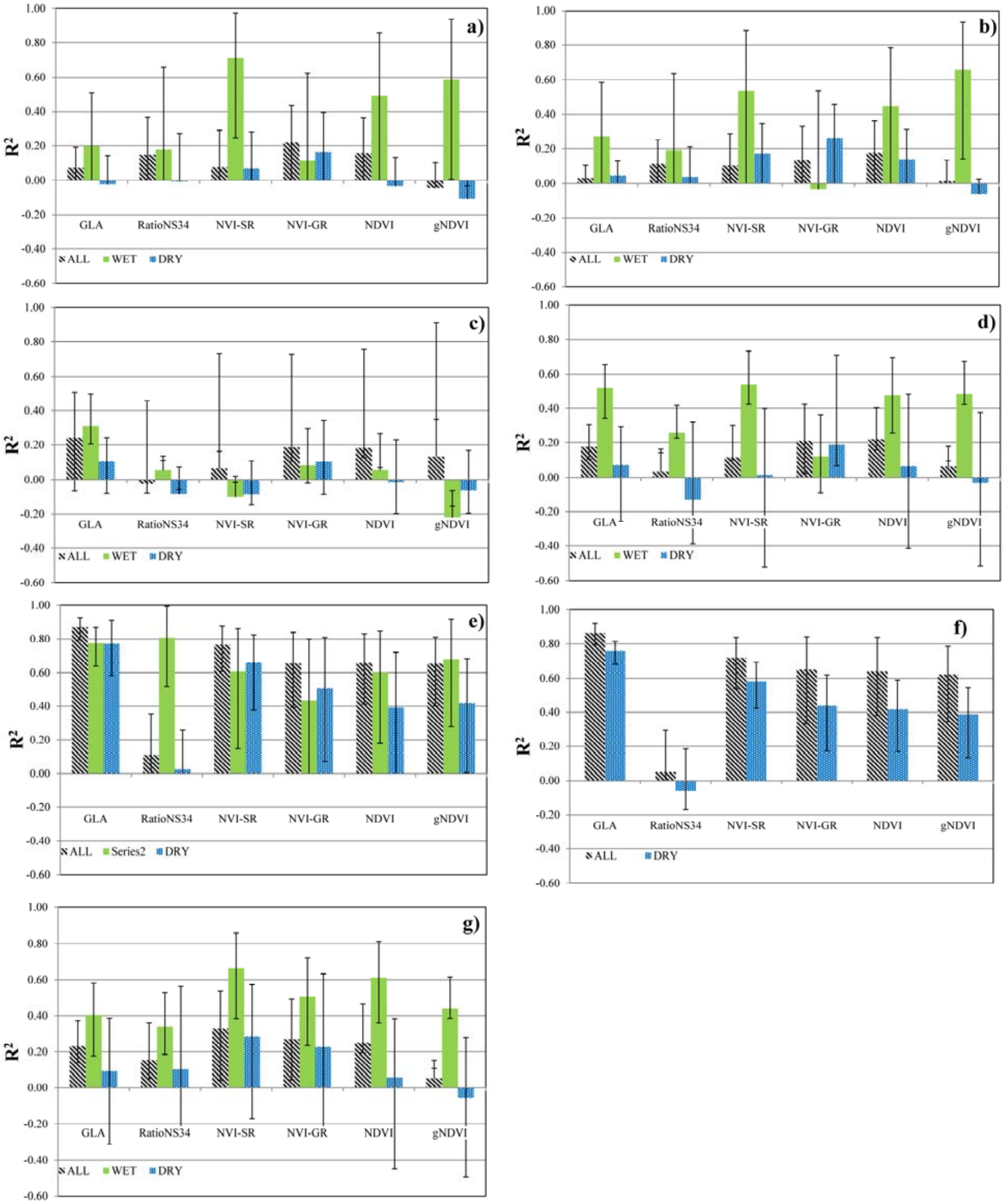

Figure 8 Bias-adjusted bootstrap point estimates of R^2 and their corresponding 95% pivotal bootstrap confidence intervals, for GAM combinations of sensor-derived indices and a) TotalBiomass, b) %BareGround, c) %Litter2D, d) %TotalVegetation2D, e) %Green3D, f) %Green2D, and g) VegetationHeight. See Table 4 for the values.